

# Rare dense solutions clusters in asymmetric binary perceptrons – local entropy via fully lifted RDT

MIHAILO STOJNIC \*

## Abstract

We study classical asymmetric binary perceptron (ABP) and associated *local entropy* (LE) as potential source of its algorithmic hardness. Isolation of *typical* ABP solutions in SAT phase seemingly suggests a universal algorithmic hardness. Paradoxically, efficient algorithms do exist even for constraint densities  $\alpha$  fairly close but at a finite distance (*computational gap*) from the capacity. In recent years, existence of rare large dense clusters and magical ability of fast algorithms to find them have been posited as the conceptual resolution of this paradox. Monotonicity or breakdown of the LEs associated with such *atypical* clusters are predicated to play a key role in their thinning-out or even complete defragmentation.

Invention of fully lifted random duality theory (fl RDT) [90, 93, 94] allows studying random structures *typical* features. A large deviation upgrade, sfl LD RDT [96, 97], moves things further and enables *atypical* features characterizations as well. Utilizing the machinery of [96, 97] we here develop a generic framework to study LE as an ABP’s atypical feature. Already on the second level of lifting we discover that the LE results are closely matching those obtained through replica methods. For classical zero threshold ABP, we obtain that LE breaks down for  $\alpha$  in  $(0.77, 0.78)$  interval which basically matches  $\alpha \sim 0.75 - 0.77$  range that currently best ABP solvers can handle and effectively indicates that LE’s behavior might indeed be among key reflections of the ABP’s computational gaps presumable existence.

**Index Terms:** Binary perceptrons; Local entropy; Random duality theory; Large deviations.

## 1 Introduction

We consider *perceptrons* – the most fundamental neural networks (NN) units and unavoidable machine learning (ML) classifying tools. As basically irreplaceable AI concepts they have been extensively studied over the last 70 years. Such studies include both looking at them as foundational parts of more complex AI architectures or as simple convenient individual models presumably indicative of more generic machine learning phenomenologies. Two classical perceptron types, *spherical* and *binary*, distinguished themselves from the early machine learning days and it is by no means an overstretching to say that determining spherical perceptron’s (zero threshold) capacity (critical data constraints density  $\alpha_c$  below which classifying is successful) is among the monumental AI breakthroughs [30, 108, 111]. In particular, as one of the very first analytical confirmations of AI’s practical potential, it crucially helped understand importance of deep analytical foundations. Moreover, continuation of such a tendency through the ensuing decades effectively ensured that modern AI is almost unimaginable without a strong theoretical support.

After initial success of [30, 108, 111], a large body of highly-sophisticated followup work [47, 48, 76, 77, 83, 87, 89, 103–105] significantly extended understanding of perceptrons often allowing shifting focus on features way beyond the classical capacities. The class of *positive* spherical perceptrons (PSP) (of which the above mentioned zero-threshold one is a special case) became particularly well understood. Strong deterministic duality and convexity as a PSP’s distinguished underlying features were recognized as main catalyst for success of analytical studies [76, 77, 83]. At the same time, lack of these features was observed as often analytically unsurpassable obstacle. This is clearly exemplified by the negative spherical perceptron (NSP) where a seemingly tiny change from a positive to a negative threshold makes things much harder [7, 16, 17,

---

\*e-mail: flatoyer@gmail.com

33, 35–38, 87] and (compared to [30, 76, 77, 83, 108, 111]) substantially more involved approaches are needed [90, 92–94].

The asymmetric binary perceptrons (ABP) that we study here are somewhat similar to NSPs as underlying strong deterministic duality is lacking. For example, simple replica symmetric predictions do not hold [47, 48, 84] and instead, more involved, replica symmetry breaking ones from [61] are needed to obtain accurate capacity characterizations [26, 32, 52, 67, 91] (somewhere in between the PSP and the ABP are the symmetric binary perceptrons (SBP) where replica symmetric predictions also do not hold but a convenient combinatorial nature of the problem still allows for simple precise characterizations [1, 2, 11, 41, 70]).

## 2 ABP algorithmic hardness

All of the above relates to perceptrons’ theoretical limits. The first next question is if these limits are practically attainable. Classical complexity theory positions ABP’s algorithmic solving as an NP problem. Due to its *worst case* nature, NP-ness rarely gives a proper explanation regarding typical solvability. Practically speaking, things are actually even worse as many excellent algorithms that perform very well in a large part of  $\alpha < \alpha_c$  interval actually exist [12, 28, 56, 59]. To put everything in concrete terms, the capacity of zero-threshold ABP is  $\alpha_c \approx 0.833$ . Known fast algorithms can solve ABP up to  $\alpha_{alg} \approx 0.75$  (sometimes even up to 0.77). Determining precisely  $\alpha_{alg}$  – the critical constraint density below which the efficient algorithms exist – is an extraordinary challenge. Characterizing ABP’s underlying structural phenomenology that actually allows for the existence of such algorithms is likely to be an equally challenging associated task. Since the current  $\alpha_{alg}$  is below  $\alpha_c$  one presumes the existence of the so-called *computational gap* (C-gap) – a key algorithmic feature already associated with a host of other (random) optimization/satisfiability problems [3, 4, 43–46, 65].

### 2.1 ABP C-gap demystification – related prior work

Over the last 20 years, a strong effort has been put forth to improve understanding of the above concepts. Whether or not the C-gap indeed exists and determining its precise value if it does exist are among key open questions. Similar questions have been studied in classes of optimization problems extending way beyond the ABP. While many excellent results have been obtained, any form of a generic resolution and a possible overall C-gap demystification remain out of reach. To give a bit of a flavor as to what kind of approaches are possible, we single out possibly the most attractive among them that focuses on studying the nature of clustered solutions. Two clustering related properties have received particular attention in recent literature: (i) *Overlap gap property* (OGP) (see, e.g., [3, 31, 39, 44–46, 65]); and (ii) *Local entropy* (LE) (see, e.g., [13, 14, 19]).

The OGP approach [3, 31, 39, 44–46, 65] attributes algorithmic efficacy to a lack of gaps in the spectrum of attainable solutions pairs (or generally  $m$ -tuples) Hamming distances. For analytically simpler but structurally presumably similar SBP alternative, it is known [19, 41] that the OGP’s presence extends well below  $\alpha_c$  (see also [42] for similar discrepancy minimization related conclusions). Assuming that OGP indeed impacts algorithmic tractability, this provides a rather strong indication of C-gap existence. On the other hand, a recent shortest path counterexample [62] disproves OGP generic hardness implication (earlier disproving examples included  $k$ -XOR ones and, due to their algebraic simplicity, have been taken as exceptions). One should however note that [62] does not disprove OGP’s relevance for particular algorithms or different optimization problems. For example, long believed OGP absence in the famous (binary) Sherrington-Kirkpatrick (SK) model [78] directly implies their solvability by polynomial algorithms [66] (related p-spin SK extensions are obtained as well [5, 6]; for earlier spherical spin-glass models related considerations see [98–101] and for importance of more sophisticated OGPs that go beyond the standard ones related to solution pairs see, e.g., [53, 60]). While the OGP role in generic algorithmic hardness remains undetermined, its presence certainly precludes existence of efficient implementations for many specific algorithmic classes [41]. Moreover, existence of practical algorithms in  $\alpha$  ranges where OGP is absent additionally strengthens its relevance for many well known problems [40, 44, 45, 71, 107].

Alternatively to the above OGP view, [54, 55] considered *typical* solutions entropy as a way of describing clustering organization and its relevance for algorithmic hardness. A complete so-called *frozen* isolation of typical solutions is predicated (and proven in [1, 2, 70] for SBP). [13, 14, 19] went further and considered

a stronger entropic refinement. They looked at *atypical* well connected clusters and proposed studying associated *local entropy* (LE). The main idea is that even though predominant typical solutions might be disconnected from each other and unreachable via local searches [1, 54, 55, 70], there may still exist rare well-connected clusters. It is then predicted that efficient algorithms find precisely such rare clusters (see, e.g., [10] for an SBP’s sampling type of justification along these lines). If such a pictorial portrayal is indeed true, then C-gap existence is likely directly related to the properties of rare clusters. Behavior of the associated local entropy (monotonicity, breakdown, negativity, etc.) is further speculated in [13, 14, 19] as a key reflection of rare clusters’ structures and its impact on algorithmic hardness. In support of such a phenomenology, [2] showed for SBP the existence of maximal diameter clusters for sufficiently small  $\alpha$ . Moreover, [2] also showed that similar clusters, albeit of linear diameter, exist even for any  $\alpha < \alpha_c$  (modulo tiny technical assumptions, [2]’s SBP results extend to ABP as well). Reconnecting back with the OGP, [23] showed that small  $\alpha$  SBP LE results scaling-wise fairly closely match the [41]’s OGP predictions (and modulo a log term the [21]’s algorithmic performance). While such a nice OGP – LE correspondence is rather convincing, establishing a definite answer as to whether or not these properties indeed crucially impact appearance of C-gaps remains a mystery. At the same time, it should be pointed out that no matter what their C-gap relevance is, these properties certainly provide deep insights into the intrinsic nature of random structures and understanding them is of independent interest as well.

## 2.2 ABP C-gap demystification – our contributions

More foundational nature of the above concepts makes them analytically much harder when compared to studying ABP’s capacity alone. As expected, the source of hardness is related to the move from studying *typical* to studying *atypical* random structures features. Such a leap is rather gigantic and, with a few exceptions, the analytical progress is often limited to statistical mechanics replica methods.

For studying *typical* features, the power of the mechanisms introduced in [90, 93, 94] suffices. Clearly, the most prominent ABP typical feature is its critical capacity  $\alpha_c$  and the machinery of [90, 93, 94] can be used to determine it [91] ( $\alpha_c$  is the critical constraint density value for which ABP associative memory functioning transitions from successful to unsuccessful phase). The same mechanisms can also be used to characterize various other ABP features associated with *typical* behavior. For example, in regimes below the capacity ( $\alpha < \alpha_c$ ), a large number of hierarchically ordered solutions (ABP memories) will be present. The *typical* solutions interrelations and entropies can be precisely determined via [90, 93, 94]. On the other hand, as we will see below, handling *atypical* features finds an fl RDT upgrade rather useful.

Following into the footsteps of [91] we here move the *typical* connection between the statistical ABP and fully lifted random duality theory (fl RDT) [80–83, 88] to a large deviation *atypical* level. Leveraging the fl RDT’s large deviation sfl LD RDT upgrade from [96, 97], we here develop a generic framework for studying ABP’s LE. Similarly to fl RDT, to have sfl LD RDT fully operational a series of underlying numerical evaluations is needed. After conducting those for zero-threshold ( $\kappa = 0$ ) ABP we uncover that already on the second level of lifting (2-sfl LD RDT), the associated worst case LE exhibits a breakdown in (0.77, 0.78)  $\alpha$  interval. This matches both the replica predictions of [14] and the range  $\alpha \sim 0.75 - 0.77$  that best ABP solvers can handle which ultimately indicates that the LEs indeed may be among the key ABP C-gaps presumable existence reflections.

### 2.2.1 Beyond ABP

As stated earlier, the ABP that we study here is a type of general perceptron concept that has dominated machine learning and neural networks studies over the last several decades. However, the methodology that we present extends way beyond perceptrons. It is easily applicable to many closely connected feasibility problems including SBPs [1, 2, 8, 10, 11, 19, 22, 23, 41, 70, 73], PSPs and NSPs [20, 29, 30, 47, 48, 57, 74, 76, 77, 83, 87, 89, 106, 109–111], and compressed sensing so-called  $\ell_1$  *sectional/strong* phase transitions [80, 85], to name a few. In addition to extension to different types of perceptrons (or single-unit nets), the extensions to multi-unit multi-layer (deep) nets are possible as well. Excellent results obtained in this direction via replica methods [18] indicate that clustering algorithmic effects do translate as the network architectures get more complex. Besides feasibility problems, without much of additional conceptual effort, our results also extend to many optimal objective seeking standard optimizations including discrepancy minimization [9, 42, 58, 64, 72, 79]

and a host of others discussed in [90, 93–95]. For example, studies of famous Hopfield and closely related Little models as well as more mathematically oriented restricted isometries [24, 25, 27, 50, 51, 68, 69, 75, 86, 93, 95, 102, 104, 105, 113] focus on the associated free energies that exhibit behavior similar to the perceptron’s one discussed above. The ground state energy values are typically achieved by a single optimal configuration which is analogous to having a *typical* solution associated with ABP’s  $\alpha_c$ . On the other hand, energetic (band) levels away from the ground state can be achieved either by a large set or by no configurations at all. This is again fully analogous to ABP, where moving below  $\alpha_c$  (to the SAT phase) allows for (exponentially) many solutions and moving above  $\alpha_c$  (to the UNSAT phase) disallows existence of any satisfiability configuration. In other words, even though these problems are unrelated to satisfiability ones per se, they do exhibit similar phase transitioning behavior. Moreover, in all these scenarios, both *typical* and *atypical* behavior can be studied via the framework introduced here.

### 3 Mathematical setup and local entropy

Following into the footsteps of [47, 48, 83, 84, 87, 91, 92], we start by recognizing that perceptrons, as key units of almost any modern machine learning concept, belong to a general class of feasibility problems

$$\begin{aligned} \mathcal{F}(G, \mathbf{b}, \mathcal{X}, \alpha): \quad & \text{find} \quad \mathbf{x} \\ & \text{subject to} \quad G\mathbf{x} \geq \mathbf{b} \\ & \quad \mathbf{x} \in \mathcal{X}, \end{aligned} \tag{1}$$

with  $G \in \mathbb{R}^{n \times n}$ ,  $\mathbf{b} \in \mathbb{R}^{m \times 1}$ , and  $\mathcal{X} \in \mathbb{R}^n$  (large *linear* regime is considered where  $m$  and  $n$  are such that  $\alpha = \lim_{n \rightarrow \infty} \frac{m}{n}$  remains constant). The above mentioned two most prominent perceptrons’ types, *spherical* and *binary* are obtained as special case of (1). Specialization to  $\mathcal{X} = \{\mathbf{x} \mid \|\mathbf{x}\|_2 = 1\} \triangleq \mathbb{S}^m$  with  $\mathbf{b} \geq 0$  gives the positive (or standard) spherical perceptron (PSP) [20, 29, 30, 47, 48, 57, 74, 76, 77, 83, 89, 106, 108, 110, 111]. The same specialization with  $\mathbf{b} < 0$  gives the negative spherical perceptron (NSP) counterpart [7, 16, 33, 35–38, 87, 92, 105]. On the other hand, specialization to  $\mathcal{X} = \{-\frac{1}{\sqrt{n}}, \frac{1}{\sqrt{n}}\}^n \triangleq \mathbb{B}^n$  gives standard or asymmetric binary perceptron (ABP) [26, 32, 47–49, 52, 59, 61, 63, 67, 70, 83, 84, 91, 105, 112] and an additional tiny change of the linear constraints,  $|G\mathbf{x}| \leq \mathbf{b}$ , gives its symmetric binary perceptron (SBP) alternative [1, 2, 8, 10, 11, 19, 22, 23, 41, 70, 73] (for a closely related discrepancy minimization problems, see, e.g., [9, 42, 58, 64, 72, 79]). To make writing easier, we consider ABP with *fixed* threshold where  $\mathbf{b} = \kappa \mathbf{1}$ ,  $\kappa \in \mathbb{R}$ , and  $\mathbf{1}$  is a column vector of all ones. Statistical context with  $G$  having independent standard normal elements is the main focus throughout the paper.

After setting

$$\xi_{ABP} = \min_{\mathbf{x} \in \mathbb{B}^n} \max_{\mathbf{y} \in \mathbb{S}_+^m} (-\mathbf{y}^T G \mathbf{x} + \kappa \mathbf{y}^T \mathbf{1}), \tag{2}$$

with  $\mathbb{B}^n$  being the vertices of the  $n$ -dimensional unit cube and  $\mathbb{S}_+^m$  being the  $m$ -dimensional unit sphere positive orthant part (i.e.,  $\mathbb{S}_+^m = \{\mathbf{y} \mid \|\mathbf{y}\|_2 = 1, \mathbf{y} \geq 0\}$ ), [83, 84, 87, 89, 91] recognized ABP’s *capacity* as

$$\begin{aligned} \alpha &= \lim_{n \rightarrow \infty} \frac{m}{n} \\ \alpha_c(\kappa) &\triangleq \max\{\alpha \mid \lim_{n \rightarrow \infty} \mathbb{P}_G(\xi_{ABP} > 0) \rightarrow 1\} \\ &= \max\{\alpha \mid \lim_{n \rightarrow \infty} \mathbb{P}_G(\mathcal{F}(G, \mathbf{b}, \mathcal{X}, \alpha) \text{ is feasible}) \rightarrow 1\}. \end{aligned} \tag{3}$$

As usual, throughout the paper we adopt the convention that subscripts next to  $\mathbb{P}$  or  $\mathbb{E}$  denote the randomness for which the statistical evaluations are done (when this is obvious from the context, specifying the subscripts is skipped).

The capacity reflects the so-called phase-transitioning nature of the underlying random ABP structure. In particular, for  $\alpha > \alpha_c$  the problem is infeasible or in the satisfiability terminology in the so-called UNSAT phase. On the other hand, for  $\alpha < \alpha_c$  it is feasible and in the SAT phase. The transition between phases happens exactly at  $\alpha_c$  where the exponentially large volume of admissible solutions shrinks so that eventually

no single point is admissible [26, 32, 52, 61, 67, 91]. Such a picture corresponds to ABP’s theoretical limit. It is manifested through the so-called *typical* behavior which by now is very well understood. On the other hand, algorithmically achieving such a limit presents a serious challenge and no known fast algorithm (say, polynomial) provably solves ABP for  $\alpha \approx \alpha_c$ . However, for sufficiently small  $\alpha$  they provably do exist. Moreover, many practical implementations exist even for  $\alpha$  not that far away from  $\alpha_c$  (for example, for zero-threshold ( $\kappa = 0$ ) ABP practically efficient algorithms can be designed even for  $\alpha \sim 0.75 - 0.77$  which indeed is not that far away from  $\alpha_c \approx 0.833$ ). So-called *atypical* features are believed to be responsible for such a picture of ABP algorithmic hardness and presumable existence of C-gaps (inability to achieve theoretical performance with fast algorithms). Namely, while the typical solutions for any  $\alpha < \alpha_c$  might be far away (disconnected) thereby portraying the problem as seemingly hard, the existence of rare (sub-dominant) clusters of solutions might still allow for design of fast algorithms. This is precisely what [13, 14] predicted while studying the local entropy of such rare clusters via replica methods. In particular, monotonicity and/or breakdown are the key local entropy features established in [13, 14] (as mentioned earlier, in support of [13, 14] predictions, modulo tiny technical assumptions [2] showed that for sufficiently small  $\alpha$  there is an exponentially large cluster of *maximal* diameter; furthermore, existence of such clusters but of *linear* diameter was also shown in [2] even for any  $\alpha < \alpha_c$ ).

The sfl RDT machinery introduced in [90, 93] can handle studying typical behaviors. To study local entropy as an atypical ABP feature an upgrade of sfl RDT [90, 93] might be useful. Companion papers [96, 97] provide such an upgrade and we show below how it can be utilized. Before we get to concretely implement mechanisms of [96, 97], we need several technical preliminaries that we discuss next.

### 3.1 ABP local entropy and associated free energy

The above mentioned ABP’s local entropy (LE) is a measure of its solutions density. Various LEs can be defined and they predominantly depend on the type of the so-called reference solution (configuration) and the associated cost functions (for more on the utilization of different LE forms, see, e.g., [13–17]). The most typical LE scenarios rely on running over all satisfiability configurations or weighing them via certain distributions as in the so-called Franz-Parisi potential [34]. For example, one can choose the reference configuration more or less uniformly among all solutions and then evaluate (scaled by  $n$ ) log of the size of the associated cluster’s part at a given Hamming distance  $d = \frac{1-\bar{\delta}}{2}$  with  $\bar{\delta}$  being the configurational overlap (for more on the role of different loss functions in reference sampling distributions and the so-called high/low margins  $\kappa$  see, e.g., [16, 17, 22, 23]). The key prediction of [13] is that if the cluster sizes/entropies are monotonically increasing with  $d$ , then solutions remain well connected through simple local fluctuations and are likely achievable by algorithms that promote such searches. A so to say *worst case* LE alternative (introduced in [14]) assumes everything as above except that the reference configuration itself need not be a solution. Two observations are in place: **(i)** even if there is no insisting that the reference configuration is a solution, it is highly likely that it will be (simply as being a center of an exponentially large cluster of solutions and particularly so if the cluster’s diameter is small); and **(ii)** if for some  $\alpha$  there is an interval of distances from each reference point without exponentially many solutions then the same holds for reference configurations that are themselves solutions. The second point effectively ensures the LE’s worst case nature. In particular, one views the worst case LE breakdown as an implication of a the lack of dense (“exponentially large”) local connectivity.

We formally write ABP’s LE as

$$S_l(\bar{\delta}) = \lim_{n, \beta, \beta_z, p \rightarrow \infty} \mathbb{E}_G \frac{\log \left( \sum_{\bar{\mathbf{x}} \in \mathbb{B}^n} \left( \sum_{\mathbf{x} \in \mathbb{B}^n, \bar{\mathbf{x}}^T \mathbf{x} = \bar{\delta}} e^{\beta \beta_z (\mathbf{1}^T h(G\mathbf{x} - \kappa) - m)} \right)^p \right)}{np}, \quad (4)$$

where standard Heaviside function  $h(\cdot)$  acts componentwise on its vector arguments. The above LE basically does the following: **(i)** first, the term in the inner parenthesis counts the number of solutions at Hamming distance  $d = \frac{1-\bar{\delta}}{2}$  from a selected reference configuration  $\bar{\mathbf{x}}$  (to be at Hamming distance  $d$  from  $\bar{\mathbf{x}}$  alternatively means to have overlap  $\bar{\delta}$  with  $\bar{\mathbf{x}}$ ); and **(ii)** second, the outer summation then selects the reference configuration

that has the largest local entropy at distance  $\bar{\delta}$ . One then recognizes that (4) can be rewritten as

$$\begin{aligned}
S_l(\bar{\delta}) &= \lim_{n,\beta,\beta_z,p \rightarrow \infty} \mathbb{E}_G \frac{\log \left( \sum_{\bar{\mathbf{x}} \in \mathbb{B}^n} \left( \sum_{\mathbf{x} \in \mathbb{B}^n, \bar{\mathbf{x}}^T \mathbf{x} = \bar{\delta}} e^{\beta \max_{\mathbf{z}} \min_{\mathbf{y} \in \mathbb{S}^m} (\beta_z (\mathbf{1}^T h(\mathbf{z} - \kappa) - m) + \mathbf{y}^T (G\mathbf{x} - \mathbf{z}))} \right)^p \right)}{np} \\
&= \lim_{n,\beta,\beta_z,p \rightarrow \infty} \mathbb{E}_G \frac{\log \left( \sum_{\bar{\mathbf{x}} \in \mathbb{B}^n} \left( \sum_{\mathbf{x} \in \mathbb{B}^n, \bar{\mathbf{x}}^T \mathbf{x} = \bar{\delta}} \max_{\mathbf{z}} e^{-\beta \max_{\mathbf{y} \in \mathbb{S}^m} (\beta_z (\mathbf{1}^T h(\mathbf{z} - \kappa) - m) - \mathbf{y}^T (G\mathbf{x} - \mathbf{z}))} \right)^p \right)}{np} \\
&= \lim_{n,\beta,\beta_z,p \rightarrow \infty} \mathbb{E}_G \frac{\log \left( \sum_{\bar{\mathbf{x}} \in \mathbb{B}^n} \left( \sum_{\mathbf{x} \in \mathbb{B}^n, \bar{\mathbf{x}}^T \mathbf{x} = \bar{\delta}} \sum_{\mathbf{z}} \left( \sum_{\mathbf{y} \in \mathbb{S}^m} e^{\beta (\beta_z (\mathbf{1}^T h(\mathbf{z} - \kappa) - m) - \mathbf{y}^T (G\mathbf{x} - \mathbf{z}))} \right)^{-1} \right)^p \right)}{np} \\
&= \lim_{n,\beta,\beta_z,p \rightarrow \infty} \mathbb{E}_G \frac{\log \left( \sum_{\bar{\mathbf{x}} \in \mathbb{B}^n} \left( \sum_{\mathbf{x} \in \mathbb{B}^n, \bar{\mathbf{x}}^T \mathbf{x} = \bar{\delta}, \mathbf{z}} \left( \sum_{\mathbf{y} \in \mathbb{S}^m} e^{\beta (\beta_z (\mathbf{1}^T h(\mathbf{z} - \kappa) - m) - \mathbf{y}^T (G\mathbf{x} - \mathbf{z}))} \right)^{-1} \right)^p \right)}{np}. \quad (5)
\end{aligned}$$

We now look at the corresponding particular type of free energy function. Consider the following Hamiltonian

$$\mathcal{H}(G) = -\mathbf{y}^T G \mathbf{x}, \quad (6)$$

and partition function

$$Z_{\bar{\mathbf{x}}}(\beta, G) = \sum_{\mathbf{x} \in \mathbb{B}^n, \bar{\mathbf{x}}^T \mathbf{x} = \bar{\delta}, \mathbf{z}} \left( \sum_{\mathbf{y} \in \mathbb{S}^m} e^{\beta (f^0(\mathbf{z}) + \mathcal{H}(G))} \right)^{-1}, \quad (7)$$

In [91] thermodynamic limit average “reciprocal” free energy was associated with (a slightly simpler)  $Z_{\bar{\mathbf{x}}}(\beta, G)$ . Here we associate the following large deviation type of reweighted variant

$$\begin{aligned}
f_{sq}(\beta) &= \lim_{n,p \rightarrow \infty} \frac{\mathbb{E}_G \log \left( \sum_{\bar{\mathbf{x}} \in \mathbb{B}^n} (Z_{\bar{\mathbf{x}}}(\beta, G))^p \right)}{np} \\
&= \lim_{n,p \rightarrow \infty} \frac{\mathbb{E}_G \log \left( \sum_{\bar{\mathbf{x}} \in \mathbb{B}^n} \left( \sum_{\mathbf{x} \in \mathbb{B}^n, \bar{\mathbf{x}}^T \mathbf{x} = \bar{\delta}, \mathbf{z}} \left( \sum_{\mathbf{y} \in \mathbb{S}^m} e^{\beta (f^0(\mathbf{z}) + \mathcal{H}(G))} \right)^{-1} \right)^p \right)}{np} \\
&= \lim_{n,p \rightarrow \infty} \frac{\mathbb{E}_G \log \left( \sum_{\bar{\mathbf{x}} \in \mathbb{B}^n} \left( \sum_{\mathbf{x} \in \mathbb{B}^n, \bar{\mathbf{x}}^T \mathbf{x} = \bar{\delta}, \mathbf{z}} \left( \sum_{\mathbf{y} \in \mathbb{S}^m} e^{\beta (f^0(\mathbf{z}) - \mathbf{y}^T G \mathbf{x})} \right)^{-1} \right)^p \right)}{np}. \quad (8)
\end{aligned}$$

Choosing  $f^0(\mathbf{z}) = \beta_z (\mathbf{1}^T h(\mathbf{z} - \kappa) - m) + \mathbf{y}^T \mathbf{z}$ , one has for the ground state

$$f_{sq}(\infty) \triangleq \lim_{\beta, \beta_z \rightarrow \infty} f_{sq}(\beta) = S_l(\bar{\delta}). \quad (9)$$

We find it useful for the ensuing considerations to utilize the following constraint free representation

$$f_{sq}(\infty) = \lim_{n,\beta,\beta_z,p \rightarrow \infty} \frac{\mathbb{E}_G \log \left( \sum_{\bar{\mathbf{x}} \in \mathbb{B}^n} \left( \sum_{\mathbf{x} \in \mathbb{B}^n, \mathbf{z}} \min_{\nu} \left( \sum_{\mathbf{y} \in \mathbb{S}^m} e^{\beta (f^0(\mathbf{z}) - \mathbf{y}^T G \mathbf{x} - \nu \bar{\mathbf{x}}^T \mathbf{x} + \nu \bar{\delta})} \right)^{-1} \right)^p \right)}{np}. \quad (10)$$

Setting  $f_{\bar{\mathbf{x}}}(\mathbf{x}) = f^0(\mathbf{z}) - \nu \bar{\mathbf{x}}^T \mathbf{x} + \nu \bar{\delta} = \beta_z (\mathbf{1}^T h(\mathbf{z} - \kappa) - m) - \mathbf{y}^T \mathbf{z} + \nu \bar{\mathbf{x}}^T \mathbf{x} - \nu \bar{\delta}$  and noting statistical equivalence of  $G$  and  $-G$ , we finally have

$$f_{sq}(\infty) = \lim_{n,\beta,\beta_z,p \rightarrow \infty} \frac{\mathbb{E}_G \log \left( \sum_{\bar{\mathbf{x}} \in \mathbb{B}^n} \left( \sum_{\mathbf{x} \in \mathbb{B}^n, \mathbf{z}} \min_{\nu} \left( \sum_{\mathbf{y} \in \mathbb{S}^m} e^{\beta (f_{\bar{\mathbf{x}}}(\mathbf{x}) + \mathbf{y}^T G \mathbf{x})} \right)^{-1} \right)^p \right)}{np}. \quad (11)$$

We now have all the ingredients to make use of the machinery from [96, 97]. The remaining presentation

is split into two parts. In the first one we formally show how the above fits within the results of [96, 97]. As usual, once such a fit is established, a sizeable set of numerical evaluations is needed to obtain concrete results. In the second part of the remaining presentation, we conduct these evaluations as well.

## 4 ABP fit within large deviation sfl RDT

One first observes that the ground state free energy from (11) is clearly a function of blirp  $\mathbf{y}^T G \mathbf{x}$ . To connect  $f_{sq}$  and blirp results from [96, 97], we follow [91, 92, 95] and start by introducing a few needed technical preliminaries. Let  $r$  be a positive integer (i.e., let  $r \in \mathbb{N}$ ) and for  $k \in \{1, 2, \dots, r+1\}$  consider real scalars  $\beta, p \geq 0$ , and  $s$ , sets  $\mathcal{X}, \bar{\mathcal{X}} \subseteq \mathbb{R}^n$ , and  $\mathcal{Y} \subseteq \mathbb{R}^m$ , function  $f_S(\cdot) : \mathbb{R}^n \rightarrow \mathbb{R}$ , and vectors  $\mathbf{p} = [\mathbf{p}_0, \mathbf{p}_1, \dots, \mathbf{p}_{r+1}]$ ,  $\mathbf{q} = [\mathbf{q}_0, \mathbf{q}_1, \dots, \mathbf{q}_{r+1}]$ , and  $\mathbf{c} = [\mathbf{c}_0, \mathbf{c}_1, \dots, \mathbf{c}_{r+1}]$  such that

$$\begin{aligned} 1 = \mathbf{p}_0 &\geq \mathbf{p}_1 \geq \mathbf{p}_2 \geq \dots \geq \mathbf{p}_r \geq \mathbf{p}_{r+1} = 0 \\ 1 = \mathbf{q}_0 &\geq \mathbf{q}_1 \geq \mathbf{q}_2 \geq \dots \geq \mathbf{q}_r \geq \mathbf{q}_{r+1} = 0, \end{aligned} \quad (12)$$

with  $\mathbf{c}_0 = 1$ ,  $\mathbf{c}_{r+1} = 0$ . Also, let  $\mathcal{U}_k \triangleq [u^{(4,k)}, \mathbf{u}^{(2,k)}, \mathbf{h}^{(k)}]$  where the elements of  $u^{(4,k)} \in \mathbb{R}$ ,  $\mathbf{u}^{(2,k)} \in \mathbb{R}^m$ , and  $\mathbf{h}^{(k)} \in \mathbb{R}^n$  are independent standard normals. Define function

$$\psi_{S,\infty}(f_S, \mathbf{p}, \mathbf{q}, \mathbf{c}, s) = \mathbb{E}_{G, \mathcal{U}_{r+1}} \frac{1}{n \mathbf{c}_r} \log \left( \mathbb{E}_{\mathcal{U}_r} \left( \dots \left( \mathbb{E}_{\mathcal{U}_3} \left( \mathbb{E}_{\mathcal{U}_2} \left( \sum_{i_3=1}^l (\mathbb{E}_{\mathcal{U}_1} Z_{S,\infty})^p \right)^{\mathbf{c}_2} \right)^{\frac{\mathbf{c}_3}{\mathbf{c}_2}} \right)^{\frac{\mathbf{c}_4}{\mathbf{c}_3}} \dots \right)^{\frac{\mathbf{c}_r}{\mathbf{c}_{r-1}}} \right), \quad (13)$$

with

$$\begin{aligned} Z_{S,\infty} &\triangleq e^{D_{0,S,\infty}} \\ D_{0,S,\infty} &\triangleq \max_{\mathbf{x} \in \mathcal{X}, \|\mathbf{x}\|_2 = x} s \max_{\mathbf{y} \in \mathcal{Y}, \|\mathbf{y}\|_2 = y} \left( \sqrt{n} f_S + \sqrt{n} y \left( \sum_{k=1}^{r+1} c_k \mathbf{h}^{(k)} \right)^T \mathbf{x} + \sqrt{n} x y^T \left( \sum_{k=1}^{r+1} b_k \mathbf{u}^{(2,k)} \right) \right) \\ b_k &\triangleq b_k(\mathbf{p}, \mathbf{q}) = \sqrt{\mathbf{p}_{k-1} - \mathbf{p}_k} \\ c_k &\triangleq c_k(\mathbf{p}, \mathbf{q}) = \sqrt{\mathbf{q}_{k-1} - \mathbf{q}_k}. \end{aligned} \quad (14)$$

With all the above technicalities in place, one can then recall on the following theorem – certainly one of the key components of sfl LD RDT.

**Theorem 1.** [97] Consider large  $n$  linear regime where  $\alpha = \lim_{n \rightarrow \infty} \frac{m}{n}$  remains constant as  $n$  grows and let  $G \in \mathbb{R}^{m \times n}$  have independent standard normal elements. Let three sets  $\mathcal{X}, \bar{\mathcal{X}} \subseteq \mathbb{R}^n$  and  $\mathcal{Y} \subseteq \mathbb{R}^m$  with unit norm elements and function  $f_{\bar{\mathbf{x}}}(\cdot) : \mathbb{R}^{3n+m} \rightarrow \mathbb{R}$  be given. Assume the complete sfl LD RDT frame from [97] and set

$$\begin{aligned} \psi_{rp} &\triangleq -\log \left( \sum_{\mathbf{x} \in \bar{\mathcal{X}}} \left( \sum_{\mathbf{x} \in \mathcal{X}} \left( \sum_{\mathbf{y} \in \mathcal{Y}} e^{\beta(f_{\bar{\mathbf{x}}} + \mathbf{y}^T G \mathbf{x})} \right)^s \right)^p \right) \quad (\text{random primal}) \\ \psi_{rd}(\mathbf{p}, \mathbf{q}, \mathbf{c}, s) &\triangleq \frac{1}{2} \sum_{k=1}^{r+1} \left( \mathbf{p}_{k-1} \mathbf{q}_{k-1} - \mathbf{p}_k \mathbf{q}_k \right) \mathbf{c}_k \omega(k; p) - \psi_{S,\infty}(f_{\bar{\mathbf{x}}}, \mathbf{p}, \mathbf{q}, \mathbf{c}, s) \quad (\text{fl random dual}). \end{aligned} \quad (15)$$

For  $\hat{\mathbf{p}}_0 \rightarrow 1$ ,  $\hat{\mathbf{q}}_0 \rightarrow 1$ , and  $\hat{\mathbf{c}}_0 \rightarrow 1$ ,  $\hat{\mathbf{p}}_{r+1} = \hat{\mathbf{q}}_{r+1} = \hat{\mathbf{c}}_{r+1} = 0$ , let the non-fixed parts of  $\hat{\mathbf{p}}$ ,  $\hat{\mathbf{q}}$ , and  $\hat{\mathbf{c}}$  satisfy

$$\frac{d\psi_{rd}(\mathbf{p}, \mathbf{q}, \mathbf{c}, s)}{d\mathbf{p}} = \frac{d\psi_{rd}(\mathbf{p}, \mathbf{q}, \mathbf{c}, s)}{d\mathbf{q}} = \frac{d\psi_{rd}(\mathbf{p}, \mathbf{q}, \mathbf{c}, s)}{d\mathbf{c}} = 0. \quad (16)$$

Then,

$$\lim_{n \rightarrow \infty} \frac{\mathbb{E}_G \psi_{rp}}{n} = \lim_{n \rightarrow \infty} \psi_{rd}(\hat{\mathbf{p}}, \hat{\mathbf{q}}, \hat{\mathbf{c}}, s) \quad (\text{strong sfl random duality}), \quad (17)$$

where  $\psi_{S,\infty}(\cdot)$  is as in (13)-(14).

*Proof.* Follows immediately from Corollary 1 in [97].  $\square$

#### 4.1 Practical realization

While the mathematical form from Theorem 1 is fairly elegant it becomes practically useful only if all associated quantities can be evaluated. As we will see below, already on the second level of lifting ( $r = 2$ ), one obtains results that are not only in an excellent agreement with replica predictions but remarkably accurately agree with the presumed BP's algorithmic hardness.

After taking binary cube sets  $\mathcal{X} = \bar{\mathcal{X}} = \mathbb{B}^n = \{-\frac{1}{\sqrt{n}}, \frac{1}{\sqrt{n}}\}^n$  and the unit sphere  $\mathcal{Y} = \mathbb{S}^m$  together with  $f_{\bar{\mathbf{x}}}(\mathbf{x}) = \beta_z(\mathbf{1}^T h(\mathbf{z} - \kappa) - m) - \mathbf{y}^T \mathbf{z} + \nu \bar{\mathbf{x}}^T \mathbf{x} - \nu \bar{\delta}$ ,  $\beta, \beta_z, p \rightarrow \infty$ , and  $\mathbf{c}_k \rightarrow \frac{c_k}{p}, k > 1$ , in Theorem 1, we observe that the *random dual* becomes

$$\begin{aligned} \psi_{rd}(\mathbf{p}, \mathbf{q}, \mathbf{c}, s) &\triangleq \frac{1}{2} \sum_{k=1}^{r+1} \left( \mathbf{p}_{k-1} \mathbf{q}_{k-1} - \mathbf{p}_k \mathbf{q}_k \right) \mathbf{c}_k - \psi_{S,\infty}(f_{\bar{\mathbf{x}}}, \mathbf{p}, \mathbf{q}, \mathbf{c}, s). \\ &= \frac{1}{2} \sum_{k=1}^{r+1} \left( \mathbf{p}_{k-1} \mathbf{q}_{k-1} - \mathbf{p}_k \mathbf{q}_k \right) \mathbf{c}_k - \frac{1}{n} \varphi(D^{(bin)}(\bar{\mathbf{x}}, s)) - \frac{1}{n} \varphi(D^{(sph)}(\bar{\mathbf{x}}, s)), \end{aligned} \quad (18)$$

where analogously to (13)-(14)

$$\varphi(D, \mathbf{c}) = \mathbb{E}_{G, \mathcal{U}_{r+1}} \frac{1}{\mathbf{c}_r} \log \left( \mathbb{E}_{\mathcal{U}_r} \left( \dots \left( \mathbb{E}_{\mathcal{U}_3} \left( \mathbb{E}_{\mathcal{U}_2} \left( \max_{\mathbf{x} \in \bar{\mathcal{X}}} \mathbb{E}_{\mathcal{U}_1} e^D \right)^{c_2} \right)^{\frac{c_3}{c_2}} \right)^{\frac{c_4}{c_3}} \dots \right)^{\frac{c_r}{c_{r-1}}} \right), \quad (19)$$

and

$$\begin{aligned} D^{(bin)}(\bar{\mathbf{x}}, s) &= \max_{\mathbf{x} \in \bar{\mathcal{X}}} \left( s \sqrt{n} \left( \left( \sum_{k=1}^{r+1} c_k \mathbf{h}^{(k)} \right)^T \mathbf{x} + \nu \bar{\mathbf{x}}^T \mathbf{x} - \nu \bar{\delta} \right) \right) \\ D^{(sph)}(s) &= \max_{\mathbf{z}} s \max_{\mathbf{y} \in \mathcal{Y}} \left( \sqrt{n} \left( \beta_z \sum_{i=1}^l (1 - h(\mathbf{z}_{i1} - \kappa)) + \mathbf{y}^T \left( \sum_{k=1}^{r+1} b_k \mathbf{u}^{(2,k)} - \mathbf{z} \right) \right) \right). \end{aligned} \quad (20)$$

One then also has

$$\begin{aligned} D^{(bin)}(\bar{\mathbf{x}}, s) &= \max_{\mathbf{x} \in \bar{\mathcal{X}}} \left( s \sqrt{n} \left( \left( \sum_{k=1}^{r+1} c_k \mathbf{h}^{(k)} \right)^T + \nu \bar{\mathbf{x}} \right) \mathbf{x} \right) = \sum_{i=1}^n \left| s \left( \left( \sum_{k=1}^{r+1} c_k \mathbf{h}_i^{(k)} \right) + \nu \bar{\mathbf{x}}_i \right) \right| \\ &= \sum_{i=1}^n \left| \left( \sum_{k=1}^{r+1} c_k \mathbf{h}_i^{(k)} \right) + \nu \bar{\mathbf{x}}_i \right| = \sum_{i=1}^n D_i^{(bin)}(\bar{\mathbf{x}}, c_k) - \nu \bar{\delta}, \end{aligned} \quad (21)$$

with

$$D_i^{(bin)}(\bar{\mathbf{x}}, c_k) = \left| \left( \sum_{k=1}^{r+1} c_k \mathbf{h}_i^{(k)} \right) + \nu \bar{\mathbf{x}}_i \right|. \quad (22)$$

Moreover,

$$\begin{aligned} \varphi(D^{(bin)}(\bar{\mathbf{x}}, s), \mathbf{c}) &= n \mathbb{E}_{G, \mathcal{U}_{r+1}} \frac{1}{\mathbf{c}_r} \log \left( \mathbb{E}_{\mathcal{U}_r} \left( \dots \left( \mathbb{E}_{\mathcal{U}_3} \left( \mathbb{E}_{\mathcal{U}_2} \left( \max_{\bar{\mathbf{x}}_i \in \mathcal{X}} \mathbb{E}_{\mathcal{U}_1} e^{D_1^{(bin)}(\bar{\mathbf{x}}, c_k)} \right)^{\mathbf{c}_2} \right)^{\frac{\mathbf{c}_3}{\mathbf{c}_2}} \right)^{\frac{\mathbf{c}_4}{\mathbf{c}_3}} \dots \right)^{\frac{\mathbf{c}_r}{\mathbf{c}_{r-1}}} \right) \\ &\quad - \nu \bar{\delta} \\ &= n \varphi(D_1^{(bin)}(\bar{\mathbf{x}}, c_k), \mathbf{c}) - \nu \bar{\delta}. \end{aligned} \quad (23)$$

We then analogously find

$$D^{(sph)}(s) = s \sqrt{n} \left\| \min \left( -\kappa \mathbf{1} + \sum_{k=2}^{r+1} b_k \mathbf{u}^{(2,k)}, 0 \right) \right\|_2. \quad (24)$$

Given statistical symmetry, for all practical purposes we can alternatively take

$$D^{(sph)}(s) = s \sqrt{n} \left\| \max \left( \kappa \mathbf{1} + \sum_{k=2}^{r+1} b_k \mathbf{u}^{(2,k)}, 0 \right) \right\|_2. \quad (25)$$

Utilization of the *square root trick* introduced in [85–87, 89] gives as in [91]’s (30) and (31)

$$D^{(sph)}(s) = s \min_{\gamma_{sq}} \left( \sum_{i=1}^m D_i^{(sph)}(b_k) + \gamma_{sq} n \right), \quad (26)$$

with

$$D_i^{(sph)}(b_k) = \frac{\max \left( \kappa + \sum_{k=2}^{r+1} b_k \mathbf{u}_i^{(2,k)}, 0 \right)^2}{4\gamma_{sq}}. \quad (27)$$

After taking  $s = -1$  one can finally connect the ground state energy,  $f_{sq}$  given in (10), and the random primal,  $\psi_{rp}(\cdot)$ , given in Theorem 1. In particular, for optimal  $\hat{\nu}$  and  $\hat{\gamma}_{sq}$  (those that maximize and minimize  $\psi_{rd}$ , respectively) we have

$$\begin{aligned} f_{sq}(\infty) &= \lim_{n, \beta, \beta_z, p \rightarrow \infty} \frac{\mathbb{E}_G \log \left( \sum_{\bar{\mathbf{x}} \in \mathbb{B}^n} \left( \sum_{\mathbf{x} \in \mathbb{B}^n, \mathbf{z}} \min_{\nu} \left( \sum_{\mathbf{y} \in \mathbb{S}^m} e^{\beta(f_{\bar{\mathbf{x}}}(\mathbf{x}) + \mathbf{y}^T G \mathbf{x})} \right)^{-1} \right)^p \right)}{np} \\ &= - \lim_{n, \beta, \beta_z, p \rightarrow \infty} \frac{\mathbb{E}_G \max_{\nu} \psi_{rp}}{n} = - \lim_{n, \beta, \beta_z, p \rightarrow \infty} \max_{\nu} \min_{\gamma_{sq}} \psi_{rd}(\hat{\mathbf{p}}, \hat{\mathbf{q}}, \hat{\mathbf{c}}, -1), \end{aligned} \quad (28)$$

where the non-fixed parts of  $\hat{\mathbf{p}}$ ,  $\hat{\mathbf{q}}$ , and  $\hat{\mathbf{c}}$  satisfy

$$\frac{d\psi_{rd}(\mathbf{p}, \mathbf{q}, \mathbf{c}, -1)}{d\mathbf{p}} = \frac{d\psi_{rd}(\mathbf{p}, \mathbf{q}, \mathbf{c}, -1)}{d\mathbf{q}} = \frac{d\psi_{rd}(\mathbf{p}, \mathbf{q}, \mathbf{c}, -1)}{d\mathbf{c}} = 0. \quad (29)$$

Relying on (18)-(27), one then finds

$$\lim_{n \rightarrow \infty} \psi_{rd}(\hat{\mathbf{p}}, \hat{\mathbf{q}}, \hat{\mathbf{c}}, -1) = \bar{\psi}_{rd}(\hat{\mathbf{p}}, \hat{\mathbf{q}}, \hat{\mathbf{c}}, \hat{\nu}, \hat{\gamma}_{sq}, -1), \quad (30)$$

where

$$\begin{aligned} \bar{\psi}_{rd}(\mathbf{p}, \mathbf{q}, \mathbf{c}, \nu, \gamma_{sq}, -1) &= \frac{1}{2} \sum_{k=1}^{r+1} \left( \mathbf{p}_{k-1} \mathbf{q}_{k-1} - \mathbf{p}_k \mathbf{q}_k \right) \mathbf{c}_k \\ &\quad + \nu \bar{\delta} - \varphi(D_1^{(bin)}(\bar{\mathbf{x}}, c_k(\mathbf{p}, \mathbf{q}))) + \gamma_{sq} - \alpha \varphi(-D_1^{(sph)}(b_k(\mathbf{p}, \mathbf{q}))). \end{aligned} \quad (31)$$

Combining (28), (30), and (31) we obtain

$$\begin{aligned} f_{sq}(\infty) &= \lim_{n, \beta, \beta_z, p \rightarrow \infty} \frac{\mathbb{E}_G \log \left( \sum_{\bar{\mathbf{x}} \in \mathbb{B}^n} \left( \sum_{\mathbf{x} \in \mathbb{B}^n, \mathbf{z}} \min_{\nu} \left( \sum_{\mathbf{y} \in \mathbb{S}^m} e^{\beta(f_{\bar{\mathbf{x}}}(\mathbf{x}) + \mathbf{y}^T G \mathbf{x})} \right)^{-1} \right)^p \right)}{np} \\ &= - \lim_{n \rightarrow \infty} \psi_{rd}(\hat{\mathbf{p}}, \hat{\mathbf{q}}, \hat{\mathbf{c}}, -1) = -\bar{\psi}_{rd}(\hat{\mathbf{p}}, \hat{\mathbf{q}}, \hat{\mathbf{c}}, \hat{\nu}, \hat{\gamma}_{sq}, -1) \\ &= - \left( \frac{1}{2} \sum_{k=1}^{r+1} \left( \hat{\mathbf{p}}_{k-1} \hat{\mathbf{q}}_{k-1} - \hat{\mathbf{p}}_k \hat{\mathbf{q}}_k \right) \hat{\mathbf{c}}_k \right. \\ &\quad \left. + \hat{\nu} \bar{\delta} - \varphi(D_1^{(bin)}(\bar{\mathbf{x}}, c_k(\hat{\mathbf{p}}, \hat{\mathbf{q}}))) + \hat{\gamma}_{sq} - \alpha \varphi(-D_1^{(sph)}(\mathbf{b}_k(\hat{\mathbf{p}}, \hat{\mathbf{q}}))) \right). \end{aligned} \quad (32)$$

We summarize the above discussion in the following theorem.

**Theorem 2.** Consider large  $n$  linear regime with  $\alpha = \lim_{n \rightarrow \infty} \frac{m}{n}$  and assume complete sfl LD RDT setup of [97]. Let  $\varphi(\cdot)$  and  $\bar{\psi}(\cdot)$  be as in (19) and (31), respectively. Also, take the “fixed” parts of  $\hat{\mathbf{p}}, \hat{\mathbf{q}},$  and  $\hat{\mathbf{c}}$  as  $\hat{\mathbf{p}}_1 \rightarrow 1, \hat{\mathbf{q}}_1 \rightarrow 1, \hat{\mathbf{c}}_1 \rightarrow 1, \hat{\mathbf{p}}_{r+1} = \hat{\mathbf{q}}_{r+1} = \hat{\mathbf{c}}_{r+1} = 0,$  and let their “non-fixed” parts satisfy

$$\begin{aligned} \frac{d\bar{\psi}_{rd}(\mathbf{p}, \mathbf{q}, \mathbf{c}, \nu, \gamma_{sq}, -1)}{d\mathbf{p}} &= \frac{d\bar{\psi}_{rd}(\mathbf{p}, \mathbf{q}, \mathbf{c}, \nu, \gamma_{sq}, -1)}{d\mathbf{q}} = \frac{d\bar{\psi}_{rd}(\mathbf{p}, \mathbf{q}, \mathbf{c}, \nu, \gamma_{sq}, -1)}{d\mathbf{c}} = 0 \\ \frac{d\bar{\psi}_{rd}(\mathbf{p}, \mathbf{q}, \mathbf{c}, \nu, \gamma_{sq}, -1)}{d\nu} &= \frac{d\bar{\psi}_{rd}(\mathbf{p}, \mathbf{q}, \mathbf{c}, \nu, \gamma_{sq}, -1)}{d\gamma_{sq}} = 0. \end{aligned} \quad (33)$$

Moreover, set

$$\begin{aligned} c_k(\hat{\mathbf{p}}, \hat{\mathbf{q}}) &= \sqrt{\hat{\mathbf{q}}_{k-1} - \hat{\mathbf{q}}_k} \\ b_k(\hat{\mathbf{p}}, \hat{\mathbf{q}}) &= \sqrt{\hat{\mathbf{p}}_{k-1} - \hat{\mathbf{p}}_k}. \end{aligned} \quad (34)$$

Then

$$\begin{aligned} f_{sq}(\infty) &= - \left( \frac{1}{2} \sum_{k=1}^{r+1} \left( \hat{\mathbf{p}}_{k-1} \hat{\mathbf{q}}_{k-1} - \hat{\mathbf{p}}_k \hat{\mathbf{q}}_k \right) \hat{\mathbf{c}}_k \right. \\ &\quad \left. + \hat{\nu} \bar{\delta} - \varphi(D_1^{(bin)}(\bar{\mathbf{x}}, c_k(\hat{\mathbf{p}}, \hat{\mathbf{q}})), \hat{\mathbf{c}}) + \hat{\gamma}_{sq} - \alpha \varphi(-D_1^{(sph)}(\bar{\mathbf{x}}, b_k(\hat{\mathbf{p}}, \hat{\mathbf{q}})), \hat{\mathbf{c}}) \right). \end{aligned} \quad (35)$$

*Proof.* Follows immediately from the previous discussion and Theorem 1.  $\square$

## 4.2 Numerical evaluations

To have the results of Theorem 2 in full power one needs to conduct underlying numerical evaluations. A particular value of  $\kappa$  is also needed to obtain concrete practically useful values. We take  $\kappa = 0$  which cor-

responds to the most famous, so-called zero-threshold, scenario. Also, as mentioned earlier, we immediately present the results for the second level of lifting since that is the lowest level where the key LE features – particularly relevant for BP algorithmic hardness and presumable existence of the associated computational gap – appear.

#### 4.2.1 $r = 2$ – second level of lifting

We have,  $r = 2$ ,  $\hat{\mathbf{p}}_0 = \hat{\mathbf{q}}_0 = 1$ ,  $\hat{\mathbf{p}}_{r+1} = \hat{\mathbf{p}}_3 = \hat{\mathbf{q}}_{r+1} = \hat{\mathbf{q}}_3 = 0$ , and  $\mathbf{c}_1 \rightarrow 1$  but in general  $\mathbf{p}_1 \neq 0$ ,  $\mathbf{p}_2 \neq 0$ ,  $\mathbf{q}_1 \neq 0$ ,  $\mathbf{q}_2 \neq 0$ , and  $\hat{\mathbf{c}}_2 \neq 0$ . Then we can write

$$\begin{aligned} \bar{\psi}_{rd}(\mathbf{p}, \mathbf{q}, \mathbf{c}, \nu, \gamma_{sq}, -1) &= \frac{1}{2}\beta^2(1 - \mathbf{p}_1\mathbf{q}_1)\mathbf{c}_1 + \frac{1}{2}\beta^2(\mathbf{p}_1\mathbf{q}_1 - \mathbf{p}_2\mathbf{q}_2)\mathbf{c}_2 \\ &+ \nu - \frac{1}{\mathbf{c}_2}\mathbb{E}_{\mathcal{U}_3} \log \left( \mathbb{E}_{\mathcal{U}_2} \left( \max_{\bar{\mathbf{x}}_1 = \pm 1} \left( \mathbb{E}_{\mathcal{U}_1} e^{\beta|\sqrt{1-\mathbf{q}_1}\mathbf{h}_1^{(1)} + \sqrt{\mathbf{q}_1 - \mathbf{q}_2}\mathbf{h}_1^{(2)} + \sqrt{\mathbf{q}_2}\mathbf{h}_1^{(3)} + \nu\bar{\mathbf{x}}_1|} \right) \right)^{\mathbf{c}_2} \right) \\ &+ \gamma_{sq} - \alpha \frac{1}{\mathbf{c}_2}\mathbb{E}_{\mathcal{U}_3} \log \left( \mathbb{E}_{\mathcal{U}_2} \left( \mathbb{E}_{\mathcal{U}_1} e^{-\beta \frac{\max(\kappa + \sqrt{1-\mathbf{p}_1}\mathbf{u}_1^{(2,1)} + \sqrt{\mathbf{p}_1 - \mathbf{p}_2}\mathbf{u}_1^{(2,2)} + \sqrt{\mathbf{p}_2}\mathbf{u}_1^{(2,3)}, 0)^2}{4\gamma_{sq}}} \right) \right)^{\mathbf{c}_2} \right). \end{aligned} \quad (36)$$

One then first finds

$$\begin{aligned} f_{(z)}^{(2)} &= \mathbb{E}_{\mathcal{U}_1} e^{\beta|\sqrt{1-\mathbf{q}_1}\mathbf{h}_1^{(1)} + \sqrt{\mathbf{q}_1 - \mathbf{q}_2}\mathbf{h}_1^{(2)} + \sqrt{\mathbf{q}_2}\mathbf{h}_1^{(3)} + \nu\bar{\mathbf{x}}_1|} \\ &= \frac{1}{2}e^{\frac{(1-\mathbf{q}_1)\beta^2}{2}} \\ &\times \left( e^{-\beta(\sqrt{\mathbf{q}_1 - \mathbf{q}_2}\mathbf{h}_1^{(2)} + \sqrt{\mathbf{q}_2}\mathbf{h}_1^{(3)} + \nu\bar{\mathbf{x}}_1)} \operatorname{erfc} \left( - \left( \beta\sqrt{1-\mathbf{q}_1} - \frac{\sqrt{\mathbf{q}_1 - \mathbf{q}_2}\mathbf{h}_1^{(2)} + \sqrt{\mathbf{q}_2}\mathbf{h}_1^{(3)} + \nu\bar{\mathbf{x}}_1}{\sqrt{1-\mathbf{q}_1}} \right) \frac{1}{\sqrt{2}} \right) \right. \\ &\left. + e^{\beta(\sqrt{\mathbf{q}_1 - \mathbf{q}_2}\mathbf{h}_1^{(2)} + \sqrt{\mathbf{q}_2}\mathbf{h}_1^{(3)} + \nu\bar{\mathbf{x}}_1)} \operatorname{erfc} \left( - \left( \beta\sqrt{1-\mathbf{q}_1} + \frac{\sqrt{\mathbf{q}_1 - \mathbf{q}_2}\mathbf{h}_1^{(2)} + \sqrt{\mathbf{q}_2}\mathbf{h}_1^{(3)} + \nu\bar{\mathbf{x}}_1}{\sqrt{1-\mathbf{q}_1}} \right) \frac{1}{\sqrt{2}} \right) \right), \end{aligned} \quad (37)$$

and

$$\mathbb{E}_{\mathcal{U}_3} \log \left( \mathbb{E}_{\mathcal{U}_2} \left( \max_{\bar{\mathbf{x}}_1 = \pm 1} \left( \mathbb{E}_{\mathcal{U}_1} e^{\beta|\sqrt{1-\mathbf{q}_1}\mathbf{h}_1^{(1)} + \sqrt{\mathbf{q}_1 - \mathbf{q}_2}\mathbf{h}_1^{(2)} + \sqrt{\mathbf{q}_2}\mathbf{h}_1^{(3)} + \nu\bar{\mathbf{x}}_1|} \right) \right)^{\mathbf{c}_2} \right) = \mathbb{E}_{\mathcal{U}_3} \log \left( \mathbb{E}_{\mathcal{U}_2} \left( \max_{\bar{\mathbf{x}}_1 = \pm 1} f_{(z)}^{(2)} \right)^{\mathbf{c}_2} \right). \quad (38)$$

Also, after setting

$$\begin{aligned} \bar{h} &= -\frac{\sqrt{\mathbf{p}_1 - \mathbf{p}_2}\mathbf{u}_1^{(2,2)} + \sqrt{\mathbf{p}_2}\mathbf{u}_1^{(2,3)} + \kappa}{\sqrt{1-\mathbf{p}_1}} \\ \bar{B} &= \frac{\mathbf{c}_2}{4\gamma_{sq}} \\ \bar{C} &= \sqrt{\mathbf{p}_1 - \mathbf{p}_2}\mathbf{u}_1^{(2,2)} + \sqrt{\mathbf{p}_2}\mathbf{u}_1^{(2,3)} + \kappa \\ f_{(zd)}^{(2,f)} &= \frac{e^{-\frac{\bar{B}\bar{C}^2}{2(1-\mathbf{p}_1)\bar{B}+1}}}{2\sqrt{2}(1-\mathbf{p}_1)\bar{B}+1} \operatorname{erfc} \left( \frac{\bar{h}}{\sqrt{4(1-\mathbf{p}_1)\bar{B}+2}} \right) \\ f_{(zu)}^{(2,f)} &= \frac{1}{2} \operatorname{erfc} \left( -\frac{\bar{h}}{\sqrt{2}} \right), \end{aligned} \quad (39)$$

we find

$$\mathbb{E}_{\mathcal{U}_3} \log \left( \mathbb{E}_{\mathcal{U}_2} \left( \mathbb{E}_{\mathcal{U}_1} e^{-\beta \frac{\max(\sqrt{1-\mathbf{p}_1}\mathbf{u}_1^{(2,1)} + \sqrt{\mathbf{p}_1 - \mathbf{p}_2}\mathbf{u}_1^{(2,2)} + \sqrt{\mathbf{p}_2}\mathbf{u}_1^{(2,3)}, 0)^2}{4\gamma_{sq}}} \right) \right)^{\mathbf{c}_2} \right) = \mathbb{E}_{\mathcal{U}_3} \log \left( \mathbb{E}_{\mathcal{U}_2} \left( f_{(zd)}^{(2,f)} + f_{(zu)}^{(2,f)} \right)^{\mathbf{c}_2} \right). \quad (40)$$

Differentiation/optimization give scaling  $\mathbf{q}_1\beta^2 \rightarrow \mathbf{q}_1^{(s)}$ ,  $\mathbf{q}_2\beta^2 \rightarrow \mathbf{q}_2^{(s)}$ , and  $\gamma_{sq} \rightarrow 0$ , and

$$\begin{aligned} f_{(z)}^{(2)} &\rightarrow e^{\frac{\beta^2 - \mathbf{q}_1^{(s)}}{2}} \left( e^{-\left(\sqrt{\mathbf{q}_1^{(s)} - \mathbf{q}_2^{(s)}} \mathbf{h}_1^{(3)} + \sqrt{\mathbf{q}_2^{(s)}} \mathbf{h}_1^{(3)} + \nu \bar{\mathbf{x}}_1\right)} + e^{\left(\sqrt{\mathbf{q}_1^{(s)} - \mathbf{q}_2^{(s)}} \mathbf{h}_1^{(3)} + \sqrt{\mathbf{q}_2^{(s)}} \mathbf{h}_1^{(3)} + \nu \bar{\mathbf{x}}_1\right)} \right) \\ &\rightarrow e^{\frac{\beta^2 - \mathbf{q}_1^{(s)}}{2}} 2 \cosh \left( \sqrt{\mathbf{q}_1^{(s)} - \mathbf{q}_2^{(s)}} \mathbf{h}_1^{(3)} + \sqrt{\mathbf{q}_2^{(s)}} \mathbf{h}_1^{(3)} + \nu \bar{\mathbf{x}}_1 \right). \end{aligned} \quad (41)$$

After observing

$$\begin{aligned} \bar{h} &= -\frac{\sqrt{\mathbf{p}_1 - \mathbf{p}_2} \mathbf{u}_1^{(2,2)} + \sqrt{\mathbf{p}_2} \mathbf{u}_1^{(2,3)} + \kappa}{\sqrt{1 - \mathbf{p}_1}} \\ \bar{B} &= \frac{\mathbf{c}_2}{4\gamma_{sq}} \rightarrow \infty \\ \bar{C} &= \sqrt{\mathbf{p}_1 - \mathbf{p}_2} \mathbf{u}_1^{(2,2)} + \sqrt{\mathbf{p}_2} \mathbf{u}_1^{(2,3)} + \kappa \\ f_{(zd)}^{(2,f)} &= \frac{e^{-\frac{\bar{B}\bar{C}^2}{2(1-\mathbf{p}_1)\bar{B}+1}}}{2\sqrt{2(1-\mathbf{p}_1)\bar{B}+1}} \operatorname{erfc} \left( \frac{\bar{h}}{\sqrt{4(1-\mathbf{p}_1)\bar{B}+2}} \right) \rightarrow 0 \\ f_{(zu)}^{(2,f)} &= \frac{1}{2} \operatorname{erfc} \left( -\frac{\bar{h}}{\sqrt{2}} \right) \rightarrow \frac{1}{2} \operatorname{erfc} \left( \frac{\sqrt{\mathbf{p}_1 - \mathbf{p}_2} \mathbf{u}_1^{(2,2)} + \sqrt{\mathbf{p}_2} \mathbf{u}_1^{(2,3)} + \kappa}{\sqrt{2}\sqrt{1-\mathbf{p}_1}} \right). \end{aligned} \quad (42)$$

and combining (36), (38), (40), (41), and (42), we find

$$\begin{aligned} -f_{sq}^{(2,f)}(\infty) &= \bar{\psi}_{rd}(\mathbf{p}, \mathbf{q}, \mathbf{c}, \gamma_{sq}, -1) \\ &= \frac{1}{2}(\beta^2 - \mathbf{p}_1 \mathbf{q}_1^{(s)}) + \frac{1}{2}(\mathbf{p}_1 \mathbf{q}_1^{(s)} - \mathbf{p}_2 \mathbf{q}_2^{(s)}) \mathbf{c}_2 - \frac{\beta^2 - \mathbf{q}_1^{(s)}}{2} \\ &\quad + \nu - \frac{1}{\mathbf{c}_2} \mathbb{E}_{\mathcal{U}_3} \log \left( \mathbb{E}_{\mathcal{U}_3} \left( \max_{\mathbf{x}_1 = \pm 1} f_{(z)}^{(2)} \right)^{\mathbf{c}_2} \right) + \gamma_{sq} - \alpha \frac{1}{\mathbf{c}_2} \mathbb{E}_{\mathcal{U}_3} \log \left( \mathbb{E}_{\mathcal{U}_3} \left( f_{(zd)}^{(2,f)} + f_{(zu)}^{(2,f)} \right)^{\mathbf{c}_2} \right) \\ &\rightarrow \frac{(1 - \mathbf{p}_1) \mathbf{q}_1^{(s)}}{2} + \frac{1}{2}(\mathbf{p}_1 \mathbf{q}_1^{(s)} - \mathbf{p}_2 \mathbf{q}_2^{(s)}) \mathbf{c}_2 \\ &\quad + \nu - \frac{1}{\mathbf{c}_2} \mathbb{E}_{\mathcal{U}_3} \log \left( \mathbb{E}_{\mathcal{U}_2} \left( \max_{\bar{\mathbf{x}}_1 = \pm 1} 2 \cosh \left( \sqrt{\mathbf{q}_1^{(s)} - \mathbf{q}_2^{(s)}} \mathbf{h}_1^{(2)} + \sqrt{\mathbf{q}_2^{(s)}} \mathbf{h}_1^{(3)} + \nu \bar{\mathbf{x}}_1 \right) \right)^{\mathbf{c}_2} \right) \\ &\quad + \gamma_{sq} - \alpha \frac{1}{\mathbf{c}_2} \mathbb{E}_{\mathcal{U}_3} \log \left( \mathbb{E}_{\mathcal{U}_2} \left( \frac{1}{2} \operatorname{erfc} \left( \frac{\sqrt{\mathbf{p}_1 - \mathbf{p}_2} \mathbf{u}_1^{(2,2)} + \sqrt{\mathbf{p}_2} \mathbf{u}_1^{(2,3)} + \kappa}{\sqrt{2}\sqrt{1-\mathbf{p}_1}} \right) \right)^{\mathbf{c}_2} \right) \\ &\rightarrow \frac{(1 - \mathbf{p}_1) \mathbf{q}_1^{(s)}}{2} + \frac{1}{2}(\mathbf{p}_1 \mathbf{q}_1^{(s)} - \mathbf{p}_2 \mathbf{q}_2^{(s)}) \mathbf{c}_2 \\ &\quad + \nu - \frac{1}{\mathbf{c}_2} \mathbb{E}_{\mathcal{U}_3} \log \left( \mathbb{E}_{\mathcal{U}_2} \left( 2 \cosh \left( \left| \sqrt{\mathbf{q}_1^{(s)} - \mathbf{q}_2^{(s)}} \mathbf{h}_1^{(2)} + \sqrt{\mathbf{q}_2^{(s)}} \mathbf{h}_1^{(3)} \right| + |\nu| \right) \right)^{\mathbf{c}_2} \right) \\ &\quad + \gamma_{sq} - \alpha \frac{1}{\mathbf{c}_2} \mathbb{E}_{\mathcal{U}_3} \log \left( \mathbb{E}_{\mathcal{U}_2} \left( \frac{1}{2} \operatorname{erfc} \left( \frac{\sqrt{\mathbf{p}_1 - \mathbf{p}_2} \mathbf{u}_1^{(2,2)} + \sqrt{\mathbf{p}_2} \mathbf{u}_1^{(2,3)} + \kappa}{\sqrt{2}\sqrt{1-\mathbf{p}_1}} \right) \right)^{\mathbf{c}_2} \right). \end{aligned} \quad (43)$$

### $\mathbf{p}$ - derivatives

For  $\mathbf{p}_1$  we first note

$$\frac{d\bar{h}}{d\mathbf{p}_1} = -\frac{1/2/\sqrt{\mathbf{p}_1 - \mathbf{p}_2} \mathbf{u}_1^{(2,2)}}{\sqrt{1 - \mathbf{p}_1}} - 1/2 \frac{\sqrt{\mathbf{p}_1 - \mathbf{p}_2} \mathbf{u}_1^{(2,2)} + \sqrt{\mathbf{p}_2} \mathbf{u}_1^{(2,3)} + \kappa}{\sqrt{1 - \mathbf{p}_1}^3}$$

$$\frac{df_{(zu)}^{(2,f)}}{d\mathbf{p}_1} = -1/2 \left( -1/\sqrt{2} \frac{d\bar{h}}{d\mathbf{p}_1} \right) \left( \frac{2}{\sqrt{\pi}} e^{-(\bar{h}/\sqrt{2})^2} \right). \quad (44)$$

We then obtain

$$\frac{d\bar{\psi}_{rd}(\mathbf{p}, \mathbf{q}, \mathbf{c}, \nu, \gamma_{sq}, -1)}{d\mathbf{p}_1} \rightarrow \frac{(\mathbf{c}_2 - 1)}{2} \mathbf{q}_1^{(s)} - \alpha \frac{1}{\mathbf{c}_2} \mathbb{E}_{\mathcal{U}_3} \frac{\mathbb{E}_{\mathcal{U}_2} \left( \mathbf{c}_2 \left( f_{(zu)}^{(2,f)} \right)^{\mathbf{c}_2 - 1} \frac{df_{(zu)}^{(2,f)}}{d\mathbf{p}_1} \right)}{\mathbb{E}_{\mathcal{U}_2} \left( f_{(zu)}^{(2,f)} \right)^{\mathbf{c}_2}}. \quad (45)$$

For  $\mathbf{p}_2$  we further note

$$\begin{aligned} \frac{d\bar{h}}{d\mathbf{p}_2} &= \frac{-1/2/\sqrt{\mathbf{p}_1 - \mathbf{p}_2} \mathbf{u}_1^{(2,2)} + 1/2/\sqrt{\mathbf{p}_2} \mathbf{u}_1^{(2,3)}}{\sqrt{1 - \mathbf{p}_1}} \\ \frac{df_{(zu)}^{(2,f)}}{d\mathbf{p}_2} &= -1/2 \left( -1/\sqrt{2} \frac{d\bar{h}}{d\mathbf{p}_2} \right) \left( \frac{2}{\sqrt{\pi}} e^{-(\bar{h}/\sqrt{2})^2} \right), \end{aligned} \quad (46)$$

and obtain

$$\frac{d\bar{\psi}_{rd}(\mathbf{p}, \mathbf{q}, \mathbf{c}, \nu, \gamma_{sq}, -1)}{d\mathbf{p}_2} \rightarrow -\frac{\mathbf{c}_2}{2} \mathbf{q}_1^{(s)} - \alpha \frac{1}{\mathbf{c}_2} \mathbb{E}_{\mathcal{U}_3} \frac{\mathbb{E}_{\mathcal{U}_2} \left( \mathbf{c}_2 \left( f_{(zu)}^{(2,f)} \right)^{\mathbf{c}_2 - 1} \frac{df_{(zu)}^{(2,f)}}{d\mathbf{p}_2} \right)}{\mathbb{E}_{\mathcal{U}_2} \left( f_{(zu)}^{(2,f)} \right)^{\mathbf{c}_2}}. \quad (47)$$

### $\mathbf{q}$ - derivatives

After setting

$$f_{(zc)}^{(2)} = 2 \cosh \left( \left| \sqrt{\mathbf{q}_1^{(s)} - \mathbf{q}_2^{(s)}} \mathbf{h}_1^{(2)} + \sqrt{\mathbf{q}_2^{(s)}} \mathbf{h}_1^{(3)} \right| + |\nu| \right), \quad (48)$$

we have (modulo continuity)

$$\begin{aligned} \frac{df_{(zc)}^{(2)}}{d\mathbf{q}_1^{(s)}} &= \text{sign} \left( \sqrt{\mathbf{q}_1^{(s)} - \mathbf{q}_2^{(s)}} \mathbf{h}_1^{(2)} + \sqrt{\mathbf{q}_2^{(s)}} \mathbf{h}_1^{(3)} \right) \left( 1/2/\sqrt{\mathbf{q}_1^{(s)} - \mathbf{q}_2^{(s)}} \mathbf{h}_1^{(2)} \right) \\ &\quad \times 2 \sinh \left( \left| \sqrt{\mathbf{q}_1^{(s)} - \mathbf{q}_2^{(s)}} \mathbf{h}_1^{(2)} + \sqrt{\mathbf{q}_2^{(s)}} \mathbf{h}_1^{(3)} \right| + |\nu| \right), \end{aligned} \quad (49)$$

and

$$\frac{d\bar{\psi}_{rd}(\mathbf{p}, \mathbf{q}, \mathbf{c}, \nu, \gamma_{sq}, -1)}{d\mathbf{q}_1^{(s)}} \rightarrow \frac{(1 - \mathbf{p}_1)}{2} + \frac{\mathbf{p}_1}{2} \mathbf{c}_2 - \frac{1}{\mathbf{c}_2} \mathbb{E}_{\mathcal{U}_3} \frac{\mathbb{E}_{\mathcal{U}_2} \left( \mathbf{c}_2 \left( f_{(zc)}^{(2)} \right)^{\mathbf{c}_2 - 1} \frac{df_{(zc)}^{(2)}}{d\mathbf{q}_1^{(s)}} \right)}{\mathbb{E}_{\mathcal{U}_2} \left( f_{(zc)}^{(2)} \right)^{\mathbf{c}_2}}. \quad (50)$$

Analogously, we then have for  $\mathbf{q}_2^{(s)}$

$$\begin{aligned} \frac{df_{(zc)}^{(2)}}{d\mathbf{q}_2^{(s)}} &= \text{sign} \left( \sqrt{\mathbf{q}_1^{(s)} - \mathbf{q}_2^{(s)}} \mathbf{h}_1^{(2)} + \sqrt{\mathbf{q}_2^{(s)}} \mathbf{h}_1^{(3)} \right) \left( -1/2/\sqrt{\mathbf{q}_1^{(s)} - \mathbf{q}_2^{(s)}} \mathbf{h}_1^{(2)} + 1/2/\sqrt{\mathbf{q}_2^{(s)}} \mathbf{h}_1^{(3)} \right) \\ &\quad \times 2 \sinh \left( \left| \sqrt{\mathbf{q}_1^{(s)} - \mathbf{q}_2^{(s)}} \mathbf{h}_1^{(2)} + \sqrt{\mathbf{q}_2^{(s)}} \mathbf{h}_1^{(3)} \right| + |\nu| \right), \end{aligned} \quad (51)$$

and

$$\frac{d\bar{\psi}_{rd}(\mathbf{p}, \mathbf{q}, \mathbf{c}, \nu, \gamma_{sq}, -1)}{d\mathbf{q}_1^{(s)}} \rightarrow -\frac{\mathbf{p}_2}{2}\mathbf{c}_2 - \frac{1}{\mathbf{c}_2}\mathbb{E}_{\mathcal{U}_3} \frac{\mathbb{E}_{\mathcal{U}_2} \left( \mathbf{c}_2 \left( f_{(zc)}^{(2)} \right)^{\mathbf{c}_2-1} \frac{df_{(zc)}^{(2)}}{d\mathbf{q}_2^{(s)}} \right)}{\mathbb{E}_{\mathcal{U}_2} \left( f_{(zc)}^{(2)} \right)^{\mathbf{c}_2}}. \quad (52)$$

### $\mathbf{c}_2$ and $\nu$ - derivatives

For  $\mathbf{c}_2$  we have

$$\begin{aligned} \frac{d\bar{\psi}_{rd}(\mathbf{p}, \mathbf{q}, \mathbf{c}, \nu, \gamma_{sq}, -1)}{d\mathbf{c}_2} &\rightarrow \frac{d}{d\mathbf{c}_2} \left( \frac{(1 - \mathbf{p}_1)\mathbf{q}_1^{(s)}}{2} + \frac{1}{2}(\mathbf{p}_1\mathbf{q}_1^{(s)} - \mathbf{p}_2\mathbf{q}_2^{(s)})\mathbf{c}_2 \right. \\ &\quad \left. + \nu - \frac{1}{\mathbf{c}_2}\mathbb{E}_{\mathcal{U}_3} \log \left( \mathbb{E}_{\mathcal{U}_2} \left( f_{(zc)}^{(2)} \right)^{\mathbf{c}_2} \right) + \gamma_{sq} - \alpha \frac{1}{\mathbf{c}_2}\mathbb{E}_{\mathcal{U}_3} \log \left( \mathbb{E}_{\mathcal{U}_2} \left( f_{(zu)}^{(2,f)} \right)^{\mathbf{c}_2} \right) \right). \\ &\rightarrow \frac{1}{2}(\mathbf{p}_1\mathbf{q}_1^{(s)} - \mathbf{p}_2\mathbf{q}_2^{(s)}) \\ &\quad + \frac{1}{\mathbf{c}_2^2}\mathbb{E}_{\mathcal{U}_3} \log \left( \mathbb{E}_{\mathcal{U}_2} \left( f_{(zc)}^{(2)} \right)^{\mathbf{c}_2} \right) - \frac{1}{\mathbf{c}_2}\mathbb{E}_{\mathcal{U}_3} \frac{\mathbb{E}_{\mathcal{U}_2} \left( \log \left( f_{(zc)}^{(2)} \right) \left( f_{(zc)}^{(2)} \right)^{\mathbf{c}_2} \right)}{\mathbb{E}_{\mathcal{U}_2} \left( f_{(zc)}^{(2)} \right)^{\mathbf{c}_2}} \\ &\quad + \frac{\alpha}{\mathbf{c}_2^2}\mathbb{E}_{\mathcal{U}_3} \log \left( \mathbb{E}_{\mathcal{U}_2} \left( f_{(zu)}^{(2,f)} \right)^{\mathbf{c}_2} \right) - \frac{\alpha}{\mathbf{c}_2}\mathbb{E}_{\mathcal{U}_3} \frac{\mathbb{E}_{\mathcal{U}_2} \left( \log \left( f_{(zu)}^{(2,f)} \right) \left( f_{(zu)}^{(2,f)} \right)^{\mathbf{c}_2} \right)}{\mathbb{E}_{\mathcal{U}_2} \left( f_{(zu)}^{(2,f)} \right)^{\mathbf{c}_2}}. \end{aligned} \quad (53)$$

For  $\nu$  we first observe (modulo continuity)

$$\frac{df_{(zc)}^{(2)}}{d\nu} = \text{sign}(\nu) 2 \sinh \left( \left| \sqrt{\mathbf{q}_1^{(s)} - \mathbf{q}_2^{(s)}} \mathbf{h}_1^{(2)} + \sqrt{\mathbf{q}_2^{(s)}} \mathbf{h}_1^{(3)} \right| + |\nu| \right), \quad (54)$$

and then

$$\frac{d\bar{\psi}_{rd}(\mathbf{p}, \mathbf{q}, \mathbf{c}, \nu, \gamma_{sq}, -1)}{d\nu} \rightarrow \bar{\delta} - \frac{1}{\mathbf{c}_2}\mathbb{E}_{\mathcal{U}_3} \frac{\mathbb{E}_{\mathcal{U}_2} \left( \mathbf{c}_2 \left( f_{(zc)}^{(2)} \right)^{\mathbf{c}_2-1} \frac{df_{(zc)}^{(2)}}{d\nu} \right)}{\mathbb{E}_{\mathcal{U}_2} \left( f_{(zc)}^{(2)} \right)^{\mathbf{c}_2}}. \quad (55)$$

A combination of (45), (47), (50), (52), (53), and (55) is sufficient to determine  $\hat{\mathbf{p}}$ ,  $\hat{\mathbf{q}}$ ,  $\hat{\mathbf{c}}$ , and  $\hat{\nu}$ . Together with  $\hat{\gamma}_{sq} \rightarrow 0$  this then suffices to determine  $\bar{\psi}_{rd}(\hat{\mathbf{p}}, \hat{\mathbf{q}}, \hat{\mathbf{c}}, \hat{\nu}, \hat{\gamma}_{sq}, -1)$  as well. The obtained results for  $\alpha = 0.77$  and  $\alpha = 0.78$  are shown in Figures 1 and 2. In Figure 1 we also show the maximal LE value,  $S_{max}$ , as a useful upper bound and an indicator how large the considered clusters are compared to their maximal size. In Table 1, the results from Figures 1 and 2 are complemented with concrete values of all relevant parameters for a particular overlap value,  $\bar{\delta} = 0.99$  (we should also add that we repeated all of the above calculations relying on modulo- $\mathbf{m}$  concepts from [96] and [97] and obtained exactly the same results as those in Figures 1 and 2 and Table 1 which implies *maximization* type of  $\mathbf{c}$  stationarity and a remarkable agreement with the same type of discovery discussed in [91, 92, 95]).

The most distinct feature concretely related to Figure 1 is the appearance of a local entropy breakdown for  $\alpha = 0.78$ . As Figure 2 further shows, for overlap values  $\bar{\delta} \geq \bar{\delta}_{c,1} \approx 0.993$ , there is no  $\nu \neq 0$  that would allow to enforce the overlap and existence of an exponentially large number of solutions at distance  $d = \frac{1-\bar{\delta}}{2}$  from any other point. This immediately implies that there are no such clusters around any solutions either (the local entropy concept studied here is the worst case variant and as such is able to exclude existence of *any* exponential clusters). This entropy breakdown trend seems to reverse only when  $\bar{\delta} \geq \bar{\delta}_{c,2} \approx 1$  (invisible in figures due to numerical instabilities of small values and being very close to 1).

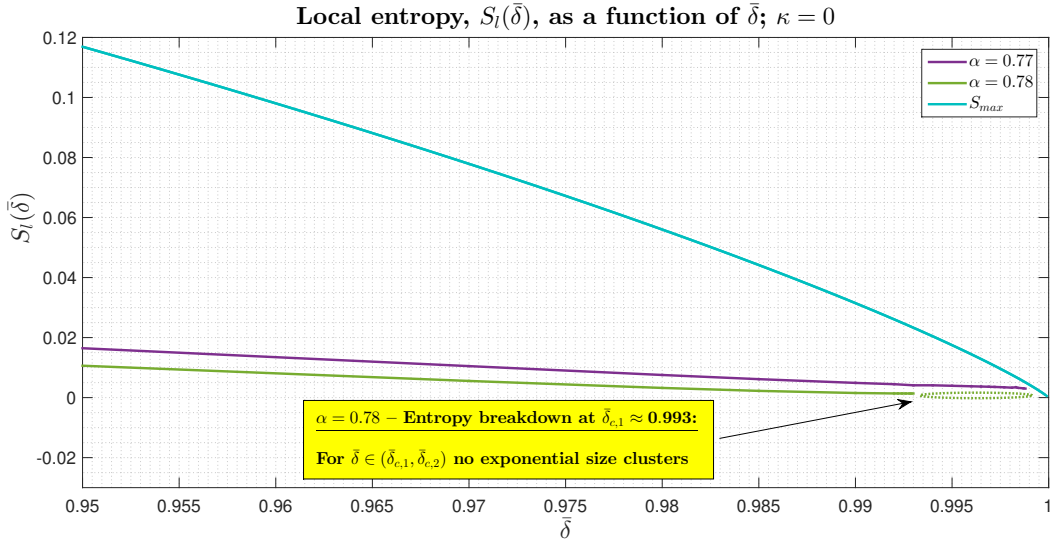


Figure 1: Local entropy breakdown

Table 1:  $r$ -sfl RDT parameters; ABP local entropy;  $\hat{c}_1 \rightarrow 1$ ;  $\kappa = 0$ ;  $n, p, \beta \rightarrow \infty$

$r$ -sfl RDT	$\alpha$	$\bar{\delta}$	$\hat{\gamma}_{sq}$	$\hat{\nu}$	$\hat{p}_2$	$\hat{p}_1$	$\hat{q}_2^{(s)} \rightarrow \hat{q}_2 \beta^2$	$\hat{q}_1^{(s)} \rightarrow \hat{q}_1 \beta^2$	$\hat{c}_2$	$S_l(\bar{\delta})$
2-sfl RDT	0.77	0.99	0	0.2258	0.6539	0.9814	0.2087	0.7924	4.86	<b>0.0049</b>
2-sfl RDT	0.78	0.99	0	0.0983	0.6536	0.9818	0.2529	0.9544	4.40	<b>0.0015</b>

It should also be noted from Figure 2 that  $\nu > 0$  remains in place for any  $\bar{\delta}$  at  $\alpha = 0.77$  implying the absence of entropy breakdown as indicated in Figure 1. This is in a perfect agreement with [14] where statistical physics replica methods were used to predicate that  $(0.77, 0.78)$   $\alpha$  window plays a key role in characterization of the worst case local entropy (it is also in a remarkable agreement with the fact that known practically feasible ABP algorithms typically have a breakdown precisely around  $\alpha \sim 0.75 - 0.77$ ). Moreover, the results shown in Figures 1 and 2 seem incredibly similar to the ones in Figure 1 in [14]. Even more remarkable is that when  $\delta q$  and  $\delta \hat{q}$  in [14]’s (B37)-(B49) are close to zero, the curves are not only visually similar but also analytically completely identical.

One should keep in mind that all the evaluations discussed above are done on the second level of lifting. While results are likely to experience tiny refinements on higher levels we do not expect major qualitative changes.

## 5 Conclusion

In a search for answers that would explain the ABP’s algorithmic hardness and presumable existence of computational gaps understanding solutions clusterings has been posited as of key importance [2, 13, 14, 39, 41]. Two problem intrinsic features, overlap gap property (OGP) and local entropy (LE), as driving forces behind specific clustering organizations, are predicated to play essential role in studying computational gaps. Even when *typical* problem solutions are isolated thereby disallowing the presence of large number of well connected clusters, there exist *atypical* exponentially large rare clusters that efficient algorithms magically discover. [13, 14] go further and predict that LE’s monotonicity or complete breakdown are directly related to the appearance of such atypicalities.

Invention of fully lifted random duality theory (fl RDT) [90, 93, 94] allowed studying random structures *typical* features (for example, ABP’s capacities and typical solutions entropies can easily be handled). A large deviation upgrade (sfl LD RDT) introduced in companion papers [96, 97] allows one to move further and

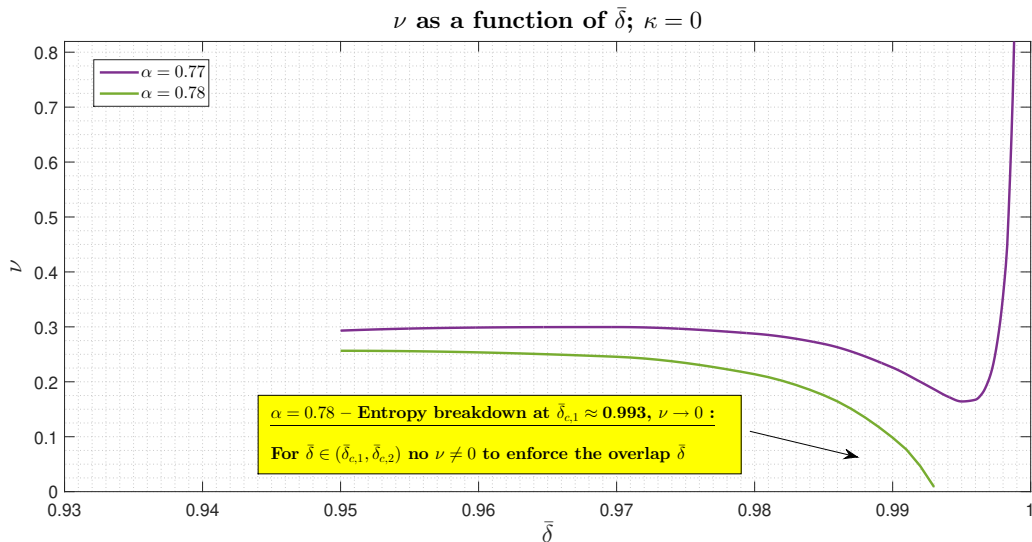


Figure 2:  $\nu$  as a function of  $\bar{\delta}$

study the *atypical* features as well. The programs developed in [96, 97] are utilized here to study ABP’s LE as an example of such atypical feature. We establish a powerful generic framework and discover that already on the second level of full lifting the results are closely matching those obtained through replica methods. In particular, we obtain that LE breaks down for  $\alpha$  in  $(0.77, 0.78)$  interval. This is both not that far away from ABP’s capacity  $\alpha_c = 0.833$  and very close to the limits of current practical algorithms ( $\alpha \sim 0.75 - 0.77$ ) which indicates that LE might indeed be associated with the existence of ABP’s computational gaps.

The introduced methodology is a generic concept and allows for various extensions beyond ABP. Many of them are related to random feasibility problems such as symmetric binary perceptrons (SBP) positive/negative spherical perceptrons, multi-layer (deep) neural nets, and *strong/sectional* compressed sensing  $\ell_1$  phase transitions. Many also relate to generic random structures such as discrepancy minimization problems and those discussed in [90, 93–95]. Obtaining concrete results for these extensions typically requires a bit of additional technical adjustment that is problem specific and will be discussed in separate papers.

## References

- [1] E. Abbe, S. Li, and A. Sly. Proof of the contiguity conjecture and lognormal limit for the symmetric perceptron. In *62nd IEEE Annual Symposium on Foundations of Computer Science, FOCS 2021, Denver, CO, USA, February 7-10, 2022*, pages 327–338. IEEE, 2021.
- [2] E. Abbe, S. Li, and A. Sly. Binary perceptron: efficient algorithms can find solutions in a rare well-connected cluster. In *STOC ’22: 54th Annual ACM SIGACT Symposium on Theory of Computing, Rome, Italy, June 20 - 24, 2022*, pages 860–873. ACM, 2022.
- [3] D. Achlioptas, A. Coja-Oghlan, and F. Ricci-Tersenghi. On the solution-space geometry of random constraint satisfaction problems. *Random Struct. Algorithms*, 38(3):251–268, 2011.
- [4] D. Achlioptas and F. Ricci-Tersenghi. On the solution-space geometry of random constraint satisfaction problems. In *Proceedings of the 38th Annual ACM Symposium on Theory of Computing, Seattle, WA, USA, May 21-23, 2006*, pages 130–139. ACM, 2006.
- [5] A. E. Alaoui, A. Montanari, and M. Sellke. Optimization of mean-field spin glasses. *The Annals of Probability*, 49(6), 2021.

- [6] A. E. Alaoui, A. Montanari, and M. Sellke. Sampling from the Sherrington-Kirkpatrick gibbs measure via algorithmic stochastic localization. In *63rd IEEE Annual Symposium on Foundations of Computer Science, FOCS 2022, Denver, CO, USA, October 31 - November 3, 2022*, pages 323–334. IEEE, 2022.
- [7] A. E. Alaoui and M. Sellke. Algorithmic pure states for the negative spherical perceptron. *Journal of Statistical Physics*, 189(27), 2022.
- [8] D. J. Altschuler. Critical window of the symmetric perceptron. 2022. available online at <http://arxiv.org/abs/2205.02319>.
- [9] R. Alweiss, Y. P. Liu, and M. Sawhney. Discrepancy minimization via a self-balancing walk. In *Proc. 53rd STOC, ACM*, pages 14–20, 2021.
- [10] A. E. Alaoui and D. Gamarnik. Hardness of sampling solutions from the symmetric binary perceptron. 2024. available online at <http://arxiv.org/abs/2407.16627>.
- [11] B. Aubin, W. Perkins, and L. Zdeborova. Storage capacity in symmetric binary perceptrons. *J. Phys. A*, 52(29):294003, 2019.
- [12] C. Baldassi, A. Braunstein, N. Brunel, and R. Zecchina. Efficient supervised learning in networks with binary synapses. *Proc. Natl. Acad. Sci. USA*, 104(26):11079–11084, 2007.
- [13] C. Baldassi, A. Ingrosso, C. Lucibello, L. Saglietti, and R. Zecchina. Subdominant dense clusters allow for simple learning and high computational performance in neural networks with discrete synapses. *Physical Review letters*, 115(12):128101, 2015.
- [14] C. Baldassi, A. Ingrosso, C. Lucibello, L. Saglietti, and R. Zecchina. Local entropy as a measure for sampling solutions in constraint satisfaction problems. *Journal of Statistical Mechanics: Theory and Experiment*, (2):021301, 2016.
- [15] C. Baldassi, C. Lauditi, E. M. Malatesta, G. Perugini, and R. Zecchina. Unveiling the structure of wide flat minima in neural networks. *Phys. Rev. Lett.*, 127:278301, Dec 2021.
- [16] C. Baldassi, E. M. Malatesta, G. Perugini, and R. Zecchina. Typical and atypical solutions in non-convex neural networks with discrete and continuous weights. 2023. available online at <http://arxiv.org/abs/2304.13871>.
- [17] C. Baldassi, E. M. Malatesta, G. Perugini, and R. Zecchina. Typical and atypical solutions in nonconvex neural networks with discrete and continuous weights. *Phys. Rev. E*, 108:024310, Aug 2023.
- [18] C. Baldassi, E. M. Malatesta, and R. Zecchina. Properties of the geometry of solutions and capacity of multilayer neural networks with rectified linear unit activations. *Phys. Rev. Lett.*, 123:170602, October 2019.
- [19] C. Baldassi, R. D. Vecchia, C. Lucibello, and R. Zecchina. Clustering of solutions in the symmetric binary perceptron. *Journal of Statistical Mechanics: Theory and Experiment*, (7):073303, 2020.
- [20] P. Baldi and S. Venkatesh. Number of stable points for spin-glasses and neural networks of higher orders. *Phys. Rev. Letters*, 58(9):913–916, Mar. 1987.
- [21] N. Bansal and J. H. Spencer. On-line balancing of random inputs. *Random Structures & Algorithms*, 57(4):879–891, 2020.
- [22] D. Barbier. How to escape atypical regions in the symmetric binary perceptron: a journey through connected-solutions states. 2024. available online at <http://arxiv.org/abs/2408.04479>.
- [23] D. Barbier, A. E. Alaoui, F. Krzakala, and L. Zdeborova. On the atypical solutions of the symmetric binary perceptron. *Journal of Physics A: Mathematical and Theoretical*, 57(19):195202, 2024.
- [24] A. Barra, G. Genovese, and F. Guerra. The replica symmetric approximation of the analogical neural network. *J. Stat. Physics*, July 2010.

- [25] A. Barra, G. Genovese, F. Guerra, and D. Tantari. How glassy are neural networks. *J. Stat. Mechanics: Theory and Experiment*, July 2012.
- [26] E. Bolthausen, S. Nakajima, N. Sun, and C. Xu. Gardner formula for Ising perceptron models at small densities. *Proceedings of Thirty Fifth Conference on Learning Theory*, PMLR, 178:1787–1911, 2022.
- [27] A. Bovier and V. Gayraud. Hopfield models as generalized random mean field models. *In mathematical aspects of spin glasses and neural networks*, *Progr. Prob.*, 41:3–89, 1998.
- [28] A. Braunstein and R. Zecchina. Learning by message passing in networks of discrete synapses. *Physical review letters*, 96(3):030201, 2006.
- [29] S. H. Cameron. Tech-report 60-600. *Proceedings of the bionics symposium*, pages 197–212, 1960. Wright air development division, Dayton, Ohio.
- [30] T. Cover. Geometrical and statistical properties of systems of linear inequalities with applications in pattern recognition. *IEEE Transactions on Electronic Computers*, (EC-14):326–334, 1965.
- [31] H. Daude, M. Mezard, T. Mora, and R. Zecchina. Pairs of sat-assignments in random boolean formulae. *Theoretical Computer Science*, 393(1):260–279, 2008.
- [32] J. Ding and N. Sun. Capacity lower bound for the Ising perceptron. *STOC 2019: Proceedings of the 51st Annual ACM SIGACT Symposium on Theory of Computing*, pages 816–827, 2019.
- [33] S. Franz, S. Hwang, and P. Urbani. Jamming in multilayer supervised learning models. *Phys. Rev. Lett.*, 123(16):160602, 2019.
- [34] S. Franz and G. Parisi. Recipes for metastable states in spin glasses. *Journal de Physique I*, 5(11):1401–1415, 1995.
- [35] S. Franz and G. Parisi. The simplest model of jamming. *Journal of Physics A: Mathematical and Theoretical*, 49(14):145001, 2016.
- [36] S. Franz, G. Parisi, M. Sevelev, P. Urbani, and F. Zamponi. Universality of the SAT-UNSAT (jamming) threshold in non-convex continuous constraint satisfaction problems. *SciPost Physics*, 2:019, 2017.
- [37] S. Franz, A. Sclocchi, and P. Urbani. Critical jammed phase of the linear perceptron. *Phys. Rev. Lett.*, 123(11):115702, 2019.
- [38] S. Franz, A. Sclocchi, and P. Urbani. Surfing on minima of isostatic landscapes: avalanches and unjamming transition. *SciPost Physics*, 9:12, 2020.
- [39] D. Gamarnik. The overlap gap property: A topological barrier to optimizing over random structures. *Proceedings of the National Academy of Sciences*, 118(41), 2021.
- [40] D. Gamarnik, A. Jagannath, and A. S. Wein. Hardness of random optimization problems for Boolean circuits, low-degree polynomials, and Langevin dynamics. *SIAM J. Comput.*, 53(1):1–46, 2024.
- [41] D. Gamarnik, E. C. Kizildag, W. Perkins, and C. Xu. Algorithms and barriers in the symmetric binary perceptron model. In *63rd IEEE Annual Symposium on Foundations of Computer Science, FOCS 2022, Denver, CO, USA, October 31 - November 3, 2022*, pages 576–587. IEEE, 2022.
- [42] D. Gamarnik, E. C. Kizildag, W. Perkins, and C. Xu. Geometric barriers for stable and online algorithms for discrepancy minimization. In *The Thirty Sixth Annual Conference on Learning Theory, COLT 2023, 12-15 July 2023, Bangalore, India*, volume 195 of *Proceedings of Machine Learning Research*, pages 3231–3263. PMLR, 2023.
- [43] D. Gamarnik, C. Moore, and L. Zdeborova. Disordered systems insights on computational hardness. *Journal of Statistical Mechanics: Theory and Experiment*, (11):115015, 2022.

- [44] D. Gamarnik and M. Sudan. Limits of local algorithms over sparse random graphs. *Proceedings of the 5th conference on innovations in theoretical computer science*, pages 369–376, 2014.
- [45] D. Gamarnik and M. Sudan. Limits of local algorithms over sparse random graphs. *Ann. Probab.*, 45(4):2353–2376, 2017.
- [46] D. Gamarnik and M. Sudan. Performance of sequential local algorithms for the random NAE-K-SAT problem. *SIAM Journal on Computing*, 46(2):590–619, 2017.
- [47] E. Gardner. The space of interactions in neural networks models. *J. Phys. A: Math. Gen.*, 21:257–270, 1988.
- [48] E. Gardner and B. Derrida. Optimal storage properties of neural networks models. *J. Phys. A: Math. Gen.*, 21:271–284, 1988.
- [49] H. Gutfreund and Y. Stein. Capacity of neural networks with discrete synaptic couplings. *J. Physics A: Math. Gen.*, 23:2613, 1990.
- [50] D. O. Hebb. *Organization of behavior*. New York: Wiley, 1949.
- [51] J. J. Hopfield. Neural networks and physical systems with emergent collective computational abilities. *Proc. Nat. Acad. Science*, 79:2554, 1982.
- [52] B. Huang. Capacity threshold for the ising perceptron. In *65th IEEE Annual Symposium on Foundations of Computer Science, FOCS 2024, Chicago, IL, USA, October 27-30, 2024*, pages 1126–1136. IEEE, 2024.
- [53] B. Huang and M. Sellke. Tight lipschitz hardness for optimizing mean field spin glasses. In *63rd IEEE Annual Symposium on Foundations of Computer Science, FOCS 2022, Denver, CO, USA, October 31 - November 3, 2022*, pages 312–322. IEEE, 2022.
- [54] H. Huang and Y. Kabashima. Origin of the computational hardness for learning with binary synapses. *Phys. Rev. E*, 90:052813, 2014.
- [55] H. Huang, K. Y. M. Wong, and Y. Kabashima. Entropy landscape of solutions in the binary perceptron problem. *Journal of Physics A: Mathematical and Theoretical*, 46(37):375002, 2013.
- [56] I. Hubara, M. Courbariaux, D. Soudry, and R. El-Yaniv and Y. Bengio. Binarized neural networks. In *Advances in Neural Information Processing Systems 29, NeurIPS 2016*, 2016.
- [57] R. D. Joseph. The number of orthants in  $n$ -space intersected by an  $s$ -dimensional subspace. *Tech. memo 8, project PARA*, 1960. Cornell aeronautical lab., Buffalo, N.Y.
- [58] N. Karmarkar, R. M. Karp, G. S Lueker, and A. M. Odlyzko. Probabilistic analysis of optimum partitioning. *Journal of Applied probability*, 23(3):626–645, 1986.
- [59] J. H. Kim and J. R. Roche. Covering cubes by random half cubes with applications to binary neural networks. *Journal of Computer and System Sciences*, 56:223–252, 1998.
- [60] E. C. Kizildag. Sharp phase transition for multi overlap gap property in ising p-spin glass and random k-SAT models. 2023. available online at <http://arxiv.org/abs/2309.09913>.
- [61] W. Krauth and M. Mezard. Storage capacity of memory networks with binary couplings. *J. Phys. France*, 50:3057–3066, 1989.
- [62] S. Li and T. Schramm. Some easy optimization problems have the overlap-gap property. 2020. available online at <http://arxiv.org/abs/2411.01836>.
- [63] S. Li, T. Schramm, and K. Zhou. Discrepancy algorithms for the binary perceptron. 2024. available online at <http://arxiv.org/abs/2408.00796>.

- [64] S. Lovett and R. Meka. Constructive discrepancy minimization by walking on the edges. *SIAM Journal on Computing*, 44(5):1573–1582, 2015.
- [65] M. Mezard, T. Mora, and R. Zecchina. Clustering of solutions in the random satisfiability problem. *Physical Review Letters*, 94:197204, 2005.
- [66] A. Montanari. Optimization of the Sherrington-Kirkpatrick hamiltonian. In *60th IEEE Annual Symposium on Foundations of Computer Science, FOCS 2019, Baltimore, Maryland, USA, November 9-12, 2019*, pages 1417–1433. IEEE Computer Society, 2019.
- [67] S. Nakajima and N. Sun. Sharp threshold sequence and universality for Ising perceptron models. *Proceedings of the 2023 Annual ACM-SIAM Symposium on Discrete Algorithms (SODA)*, pages 638–674, 2023.
- [68] L. Pastur and A. Figotin. On the theory of disordered spin systems. *Theory Math. Phys.*, 35(403-414), 1978.
- [69] L. Pastur, M. Shcherbina, and B. Tirozzi. The replica-symmetric solution without the replica trick for the Hopfield model. *Journal of Statistical Physics*, 74(5/6), 1994.
- [70] W. Perkins and C. Xu. Frozen 1-RSB structure of the symmetric Ising perceptron. *STOC 2021: Proceedings of the 53rd Annual ACM SIGACT Symposium on Theory of Computing*, pages 1579–1588, 2021.
- [71] M. Rahman and B. Virag. Local algorithms for independent sets are half-optimal. *Annals of Probability*, 45(3), 2017.
- [72] T. Rothvoss. Constructive discrepancy minimization for convex sets. *SIAM Journal on Computing*, 46(1):224–234, 2017.
- [73] A. Sah and M. Sawhney. Distribution of the threshold for the symmetric perceptron. In *2023 IEEE 64th Annual Symposium on Foundations of Computer Science (FOCS)*, pages 2369–2382, 2023.
- [74] L. Schläfli. *Gesammelte Mathematische Abhandlungen I*. Basel, Switzerland: Verlag Birkhauser, 1950.
- [75] M. Shcherbina and B. Tirozzi. The free energy of a class of Hopfield models. *Journal of Statistical Physics*, 72(1/2), 1993.
- [76] M. Shcherbina and B. Tirozzi. On the volume of the intrersection of a sphere with random half spaces. *C. R. Acad. Sci. Paris. Ser I*, (334):803–806, 2002.
- [77] M. Shcherbina and B. Tirozzi. Rigorous solution of the Gardner problem. *Comm. on Math. Physics*, (234):383–422, 2003.
- [78] D. Sherrington and S. Kirkpatrick. Solvable model of a spin glass. *Phys. Rev. Letters*, 35:1792–1796, 1972.
- [79] J. Spencer. Six standard deviations suffice. *Transactions of the American mathematical society*, 289(2):679–706, 1985.
- [80] M. Stojnic. Various thresholds for  $\ell_1$ -optimization in compressed sensing. available online at <http://arxiv.org/abs/0907.3666>.
- [81] M. Stojnic. A simple performance analysis of  $\ell_1$ -optimization in compressed sensing. *ICASSP, International Conference on Acoustics, Signal and Speech Processing*, April 2009.
- [82] M. Stojnic.  $\ell_1$  optimization and its various thresholds in compressed sensing. *ICASSP, IEEE International Conference on Acoustics, Signal and Speech Processing*, pages 3910–3913, 14-19 March 2010. Dallas, TX.

- [83] M. Stojnic. Another look at the Gardner problem. 2013. available online at <http://arxiv.org/abs/1306.3979>.
- [84] M. Stojnic. Discrete perceptrons. 2013. available online at <http://arxiv.org/abs/1303.4375>.
- [85] M. Stojnic. Lifting  $\ell_1$ -optimization strong and sectional thresholds. 2013. available online at <http://arxiv.org/abs/1306.3770>.
- [86] M. Stojnic. Lifting/lowering Hopfield models ground state energies. 2013. available online at <http://arxiv.org/abs/1306.3975>.
- [87] M. Stojnic. Negative spherical perceptron. 2013. available online at <http://arxiv.org/abs/1306.3980>.
- [88] M. Stojnic. Regularly random duality. 2013. available online at <http://arxiv.org/abs/1303.7295>.
- [89] M. Stojnic. Spherical perceptron as a storage memory with limited errors. 2013. available online at <http://arxiv.org/abs/1306.3809>.
- [90] M. Stojnic. Bilinearly indexed random processes – *stationarization* of fully lifted interpolation. 2023. available online at <http://arxiv.org/abs/2311.18097>.
- [91] M. Stojnic. Binary perceptrons capacity via fully lifted random duality theory. 2023. available online at <http://arxiv.org/abs/2312.00073>.
- [92] M. Stojnic. Fl rdt based ultimate lowering of the negative spherical perceptron capacity. 2023. available online at <http://arxiv.org/abs/2312.16531>.
- [93] M. Stojnic. Fully lifted interpolating comparisons of bilinearly indexed random processes. 2023. available online at <http://arxiv.org/abs/2311.18092>.
- [94] M. Stojnic. Fully lifted random duality theory. 2023. available online at <http://arxiv.org/abs/2312.00070>.
- [95] M. Stojnic. Studying Hopfield models via fully lifted random duality theory. 2023. available online at <http://arxiv.org/abs/2312.00071>.
- [96] M. Stojnic. Fully lifted *blirp* interpolation – a large deviation view. 2025. available online at arxiv.
- [97] M. Stojnic. A large deviation view of *stationarized* fully lifted *blirp* interpolation. 2025. available online at arxiv.
- [98] E Subag. The complexity of spherical p-spin models - A second moment approach. *Ann. Probab.*, 45:3385 – 3450, 2017.
- [99] E Subag. The geometry of the gibbs measure of pure spherical spin glasses. *Inventiones Mathematicae*, 210:135 – 209, 2017.
- [100] E Subag. Following the ground states of full-rsb spherical spin glasses. *Comm. Pure Appl. Math.*, 74:1021–1044, 2021.
- [101] E Subag. Free energy landscapes in spherical spin glasses. *Duke Math. J.*, 173:1291 – 1357, 2024.
- [102] M. Talagrand. Rigorous results for the Hopfield models with many patterns. *Prob. Theor. Rel. Fields*, 110:109–176, 1998.
- [103] M. Talagrand. *The Generic Chaining*. Springer-Verlag, 2005.
- [104] M. Talagrand. *Mean field models and spin glasse: Volume II*. A series of modern surveys in mathematics 55, Springer-Verlag, Berlin Heidelberg, 2011.

- [105] M. Talagrand. *Mean field models and spin glasses: Volume I*. A series of modern surveys in mathematics 54, Springer-Verlag, Berlin Heidelberg, 2011.
- [106] S. Venkatesh. Epsilon capacity of neural networks. *Proc. Conf. on Neural Networks for Computing, Snowbird, UT*, 1986.
- [107] A. S Wein. Optimal low-degree hardness of maximum independent set. *Mathematical Statistics and Learning*, 4(3):221–251, 2022.
- [108] J. G. Wendel. A problem in geometric probability. *Mathematica Scandinavica*, 1:109–111, 1962.
- [109] J. G. Wendel. A problem in geometric probability. *Mathematics Scandinavia*, 11:109–111, 1962.
- [110] R. O. Winder. Single stage threshold logic. *Switching circuit theory and logical design*, pages 321–332, Sep. 1961. AIEE Special publications S-134.
- [111] R. O. Winder. *Threshold logic*. Ph. D. dissertation, Princeton University, 1962.
- [112] C. Xu. Sharp threshold for the Ising perceptron model. *Ann. Probab.*, 43(5):2399–2415, 2021.
- [113] J. Y. Zhao. The Hopfield model with superlinearly many patterns. 2011. available online at <http://arxiv.org/abs/1108.4771>.